AGU PUBLICATIONS

JGR

Journal of Geophysical Research: Oceans

RESEARCH ARTICLE

10.1002/2016JC012580

Interannual surface salinity on Northwest Atlantic shelf

Semyon A. Grodsky[1], Nicolas Reul[2], Bertrand Chapron[2], James A. Carton[1], and Frank O. Bryan[3]

[1]Department of Atmospheric and Oceanic Science, University of Maryland, College Park, Maryland, USA, [2]Institut Francais pour la Recherche et l'Exploitation de la Mer, Plouzane, France, [3]Climate and Global Dynamics Laboratory, National Center for Atmospheric Research, Boulder, Colorado, USA

Key Points:
- Spatially coherent interannual SSS encompasses the Scotia-to-Hatteras NW Atlantic shelf region
- Salty and warm events occur coincident with east-southeast wind anomalies and weakening of both branches of the Scotian Shelf Current
- Salt advection by anomalous SSC is the primary driver that regulates the transport of fresh/cold water from high latitudes

Correspondence to:
S. A. Grodsky,
senya@atmos.umd.edu

Citation:
Grodsky, S. A., N. Reul, B. Chapron, J. A. Carton, and F. O. Bryan (2017), Interannual surface salinity on Northwest Atlantic shelf, *J. Geophys. Res. Oceans*, *122*, 3638–3659, doi:10.1002/2016JC012580.

Received 23 NOV 2016
Accepted 20 MAR 2017
Accepted article online 23 MAR 2017
Published online 4 MAY 2017

Abstract Sea surface salinity (SSS) from the Aquarius and SMOS satellite missions displays a steady increase of ~1 psu over the entire northwestern Atlantic shelf south of Nova Scotia during 2011–2015. Put in the context of longer ocean profile data, the results suggest that mixed layer salinity and temperature north of the Gulf Stream experience positively correlated shelf-wide interannual oscillations (1 psu/2°C). Salty and warm events occur coincident with anomalous easterly-southeasterly winds and Ekman transport counteracting the mean southwestward shelf currents. They are coincident with weakening of both branches of the Scotian Shelf Current (SSC), but only moderately correlate with shifts of the Gulf Stream North Wall. This suggests that salt advection by anomalous SSC acting on the mean salinity gradient is the primary driver regulating the transport of fresh/cold water from high latitudes. The advection mechanism imposes a connectedness of the larger-scale interannual variability in this region and its tie to atmospheric oscillations. In the second part, an analysis of 15 year-long numerical simulations is presented which show eight interannual salinity oscillations (positive and negative). Six of these are driven by horizontal advection by slow varying currents (>2 months), while two events are driven by horizontal eddy advection (<2 months). In line with observations, salt/warm model events correspond to anomalously weak SSC, correlate with southeasterly wind anomaly, and confirm that interannual horizontal salt advection drives interannual salinity. Indeed, vertical exchanges provide negative feedback, while interannual horizontal diffusion and the net surface salt flux anomalies are small.

1. Introduction

This paper explores interannual salinity along the shelf and slope sea of the northwestern (NW) Atlantic using the new large-scale perspective made available by satellite sea surface salinity (SSS) [e.g., *Lagerloef et al*., 2012; *Reul et al*., 2014a]. The study extends from Cape Hatteras north to the tail of the Grand Banks over a region where recent ocean changes are receiving much attention. Sea level variations [*Ezer and Atkinson*, 2014], Gulf Stream position shifts [*Andres*, 2016], and a high recent rate in upper ocean heating [*Gawarkiewicz et al*., 2012; *Mills et al*., 2013] are all observed, with differing potential impacts on the circulation, ecosystems, and coastal populations. Regional salinity change is also under study [*Townsend et al*., 2015; *Li et al*., 2014; *Feng et al*., 2016], mainly using in situ observations, with ecosystem implications tied to changing nutrients and factors controlling ocean acidification rates. These studies identify the need for spatially resolved and shelf-wide salinity observations. Such data would help to fill a large gap in monitoring of the hydrographic change due to variable downcoast advection, its fate, and its controls.

The continental shelf in the NW Atlantic hosts a productive marine ecosystem that supports the local coastal economy. This region displays significant interannual variability in biomass, which is linked to physical processes such as interannual winds and their impacts on currents, as well as the partitioning between Atlantic and Labrador Current source waters entering the shelf [e.g. *Greene et al*., 2013; *Saba et al*., 2015]. While there is a contribution from coastal freshwater discharge, the majority of freshwater and nutrient inflow to this shelf system is provided by alongshelf southwestward currents [*Townsend et al*., 2006]. This suggests that interannual salinity variations may serve as an indirect indicator of the changing shelf biology. In this study, we use a combination of analysis of observations and numerical simulation to show the importance of wind-driven horizontal advection in regulating the interannual variations in salinity on this shelf.

Relatively cold and fresh coastal-trapped NW Atlantic shelf water flows equatorward and is fed from high latitude freshwater sources [*Chapman et al*., 1986; *Loder et al*., 1998a,1998b]. Both historical data and ocean models show interannual variations in the shelf hydrography [*Loder et al*., 2001]. Observed interannual variations in temperature and salinity reach about 4.5C and 0.7psu, respectively, and may be associated in part with corresponding variations in the input and water mass properties of the Labrador Current [*Petrie and Drinkwater*, 1993]. This water is transported along the Scotian Shelf by the inshore and offshore branches of the southwestward Scotian Shelf Current (SSC) (see circulation schemes in Figure 1 of *Saba et al*. [2015] and Figure 5.4 of *Townsend et al*. [2006]). The offshore branch of this southwestward flow is fed by Labrador Slope Water, which circulates anticyclonically around the Grand Banks [*Csanady and Hamilton*, 1988]. The

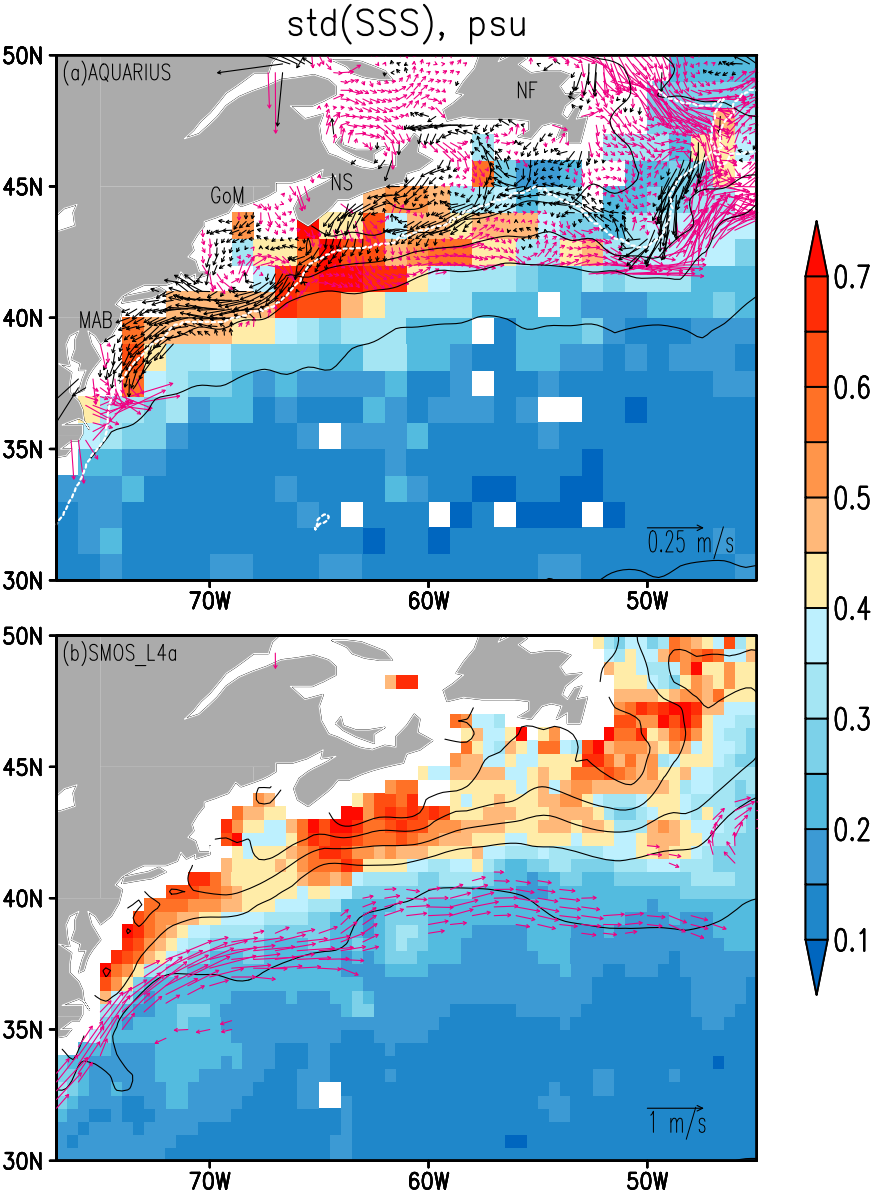

Figure 1. Standard deviation of anomalous monthly SSS (psu) August 2011 to July 2015 from (a) Aquarius (v4.0) (b) SMOS (L4a). Corresponding annual climatologic SSS contours (32–37 psu, CI = 1psu) are overlain. Annual mean shelf currents (OSCAR, magenta/black corresponds to eastward/westward, respectively) and 1000 m depth contour (white-dashed, a proxy for the shelf boundary) are shown in Figure 1a, currents>25cm/s are shown in Figure 1b. The locations: Newfoundland (NF), Nova Scotia (NS), Gulf of Maine (GoM), Mid-Atlantic Bight (MAB), are indicated in Figure 1a.

inshore branch is fed by a mixture of waters from the Labrador Shelf and Gulf of St. Lawrence [*Houghton and Fairbanks*, 2001].

A number of competing ideas have been proposed regarding the mechanisms of variability of the wind-driven circulation on the Scotian Shelf. *Li et al*. [2014] have found that the inshore branch of the SSC is regulated by interannual variations in the alongshore winds, which modify the cross-shore sea level gradient via Ekman processes, thus amplifying the along wind component of the geostrophically balanced coastal current. According to this mechanism, stronger southwesterly winds weaken the prevailing southwestward inshore SSC branch, whereas weaker southwesterly winds strengthen the southwestward inshore SSC branch. This wind-induced flow variability influences the transport of low-salinity water from the Gulf of St. Lawrence, explaining the presence of interannual variations in surface salinity within the region [*Li et al*., 2014]. In contrast, the diagnostic analysis of observations by *Feng et al*. [2016] indicates that increased southwestward flow on the Scotian Shelf (and thus a stronger inshore branch of the SSC) is related to increased cross-shore (northwesterly) winds, suggestive of a contribution by alongshore Ekman transport.

Alternatively, *Petrie and Drinkwater* [1993] have argued that the variations in the westward transport of Labrador Slope Water from the Newfoundland region along the shelfbreak (including the downstream offshore SSC branch) play a major role in the determination of the water mass properties in the Scotian Shelf-Gulf of Maine region. The Labrador Slope Water transport is strongly modulated by anomalies of zonal winds driven by the relative strengths of two large-scale atmospheric surface pressure cells: the Icelandic Low and the Azores High. The North Atlantic Oscillation Index, NAO, [*Hurrell et al*., 2003] depends on the difference between these two. During prolonged periods of a positive phase of the NAO, a lesser volume of the colder and fresher Labrador Current water turns southwest and mixes with the warmer and saltier shelf and slope waters downstream. In contrast, during a negative phase of the NAO a greater volume of Labrador Current water veers to the west along the shelfbreak, thus leading to greater cooling and freshening of the shelf and slope waters downstream [*Petrie and Drinkwater*, 1993; *Greene et al*., 2013]. Due to variations in the Labrador Current partitioning, the thermohaline properties of the eastern Canadian continental shelf water respond to sustained periods (several years) of weaker and stronger winter NAO leading to a dipole-like pattern. "The warm, salty (or cold, fresh) conditions prevail on the Newfoundland-Labrador Shelf, the eastern Scotian Shelf, and the Gulf of St. Lawrence during periods of negative (or positive) NAO phase. The opposite response is seen on the central and western Scotian Shelf and in the Gulf of Maine" [*Petrie*, 2007].

Westward transport of Labrador Slope Water along the shelf edge carries these anomalies down toward the Middle Atlantic Bight (MAB). They are observed as positively correlated interannual fluctuations of upper ocean temperature, salinity, and currents along the repeating Oleander ship transects [*Flagg et al*., 2006]. In these records, the temperature and salinity variations are positively correlated and coherent all across the shelf and slope out to the Gulf Stream. Although the velocity variability is not as coherent, there is a clear relationship between the interannual current variations and the water properties indicating that the hydrographic variability is largely due to interannual variations in advective effects. These anomalies become enhanced along the shelf-slope front extending from the tail of the Grand Banks to Cape Hatteras and separating colder and less saline continental shelf waters from warmer and more saline slope waters. It is largely a density-compensated front with strong seasonal variability in T and S (5°C and 2 psu), both maximum in summer [e.g., *Linder and Gawarkiewicz*, 1998]. These shelf-slope front anomalies take about 4 years to propagate from the tail of the Grand Banks in the east to Cape Hatteras in the west [*Bisagni et al*., 2009], in turn suggesting that the same sign of anomalous temperature and salinity should be observed south of the Scotian Shelf if the anomalies persist for longer than 4 years. Being largely driven by wind impacts on the shelf circulation, the resulting SST anomalies can feedback on the atmosphere on quasi-local [*Wills et al*., 2016] and basin-wide [e.g., *Wen et al*., 2005] scales, thus leading to coupled atmosphere-ocean interactions.

There is a systematic reduction in the southward transport of high latitude waters from about 0.7 Sv on the Scotian Shelf to lesser values as water passes the Gulf of Maine and enters the MAB [*Loder et al*., 1998b]. Regardless of the southward reduction, the horizontal transport remains a dominant factor governing interannual salinity further south even in estuaries like the Long Island Sound where anomalous coastal freshwater discharge explains only 25% of the variance of the salinity anomaly [*Lee and Lwiza*, 2005]. Expecting that along shelf reduction in the southwestward freshwater transport is accompanied by the associated reduction in cold water transport, one may note that even in the MAB, the horizontal heat transport remains the major term balancing the positive 10 Wm^{-2} net surface heat flux into the ocean [*Beardsley and Boicourt*, 1981;

Lentz, 2010]. In comparison with the mixed layer heat budget, the horizontal advection is expected to play even a greater role for the mixed layer salt budget [e.g., *Foltz et al*., 2004]. Because SSS anomalies are not damped by air-sea feedbacks, it is perhaps not surprising for such SSS anomalies to persist and be transported away from their originations. Moreover, near-surface fresh layer present on the shelf is additionally preserved by the damping effect of the barrier layer on turbulent exchanges with saltier water below [*Liu et al*., 2009].

Alongshelf equatorward transport of subpolar waters is accompanied by complex cross-shelf exchanges between the shelf water and the Slope Sea. The latter is a buffer zone separating the Gulf Stream from the shelf, in which subpolar and subtropical waters mix [e.g., *Rossby*, 1999]. Interannual variations of the Gulf Stream north wall latitude (GSNW) [*Taylor and Stephens*, 1998] are regulated by the large-scale pattern of wind curl over the North Atlantic through interannual changes in the strength and position of the Icelandic low and Azores high atmospheric surface pressure systems [e.g., *Taylor and Stephens*, 1998; *Joyce et al*., 2000; *Sanchez-Franks et al*., 2016]. The GSNW may serve as a proxy for variable slope water properties. Indeed, it moderately correlates with interannual salinity even in the inner shelf regions like the Long Island Sound ($r=0.4$ at zero lag) [*Lee and Lwiza*, 2005].

Studies of interannual changes in the NW Atlantic shelf have been relying on in situ oceanographic data so far. Because the shelf is a highly variable ocean zone that extends over a vast area, the best way to monitor its variability is provided by satellite sensors as has been demonstrated using ocean color data [e.g., *Schollaert et al*., 2004]. Although satellite sea surface temperature (SST) has been available since 1982 [*Reynolds et al*., 2007], the SSS, which is principal to the shelf studies, has become available only since the early 2010s. Recently two instruments, the Soil Moisture and Ocean Salinity (SMOS, 2010-onward) [e.g., *Boutin et al*., 2012; *Reul et al*., 2014a] and the US/Argentina Aquarius/SACD (2011–2015) [*Lagerloef et al*., 2012] have begun providing SSS measurements from space, offering a more direct approach to track temporally and spatially varying shelf water characteristics. Both instruments, Aquarius and SMOS, demonstrate good regional performance and are able to detect spatial gradients associated with the mean and eddy salinity fields of the Gulf Stream system [*Reul et al*., 2014b; *Umbert et al*., 2015]. Here we use observations of satellite SSS and SST together with ancillary observations to better identify spatial patterns of a significant salinification of the NW Atlantic shelf in the Scotian-to-Hatteras latitude band from the summer-fall of 2011 through 2015 and explore the potential causes of this change. Our focus is on the broader perspective that the combined satellite-model approach affords.

2. Data and Methods

For this study, we rely on two satellite-based SSS data sets. The first is monthly Level 3 gridded Aquarius SSS (version 4.0), which spans 4 years from August 2011 through June 2015. It is obtained from the NASA Jet Propulsion Laboratory Physical Oceanography Distributed Active Archive Center on a $1^\circ \times 1^\circ$ grid and has a characteristic accuracy of about 0.2 psu for monthly averages [see *Lee*, 2016 for more detailed accuracy analysis]. The second is the monthly Level 4 (L4a) European Space Agency Soil Moisture and Ocean Salinity (SMOS) SSS, which spans 6 years from 2010 through April 2016. It is obtained from the Centre d'Expertise IFREMER du CATDS-Ocean Salinity on a $0.5^\circ \times 0.5^\circ$ grid. Because the accuracy decreases over cold water and near coasts, the SMOS SSS are adjusted by applying a large-scale bias correction using monthly optimally interpolated in situ profile data produced by the French Coriolis Data Archiving Center In Situ Analysis System [*Reul et al*., 2015].

Both satellite salinity missions operate in the L-band (1.4 GHz) where water emissivity depends on salinity. The background Earth thermal radiation in this band is almost seven orders of magnitude weaker than in the infrared bands widely used for SST remote sensing. Such weak L-band radiation makes SSS retrieval challenging, especially in high-latitude cold water conditions where L-band thermal radiation is less sensitive to SSS. This leads to some remaining biases in retrieved SSS that amplify poleward and have significant seasonal variations [see, e.g., *Melnichenko et al*., 2016 for bias illustration]. Although satellite SSS is reasonably close to quasi-synchronous in situ measurements in the tropics [e.g., *Grodsky et al*., 2012], employing satellite SSS at higher latitudes is still subject to limitations due to the seasonally dependent bias. Fortunately, SSS anomalies relative to SSS monthly climatology are free from this seasonal bias that is removed along with the real seasonal cycle. Anomalous (or nonseasonal) satellite SSS, which is used in this paper, has

higher accuracy and area of its applicability may be extended beyond the tropics into the midlatitude ocean [*Boutin et al*., 2016; *Lee*, 2016].

Satellite SSS records are not long enough to resolve interannual processes. Longer, but less frequently sampled records are available from in situ measurements. We examine two such data-only analyses. The Japan Agency for Marine-Earth Science and Technology (JAMSTEC) employs two-dimensional optimal interpolation of Argo floats, ocean mooring data, and CTD casts on pressure surfaces for monthly analysis of temperature and salinity on a global $1^\circ \times 1^\circ$ grid from January 2001-ongoing [*Hosoda et al*., 2008]. The Met Office Hadley Centre EN4 (version 4.1.1) global $1^\circ \times 1^\circ$ ocean temperature and salinity monthly objective analysis of *Good et al*. [2013] covers the longer period 1900 to present (from which we focus only on the shorter data coincident with satellite altimetry observations since 1993). It uses the World Ocean Database 2009 as a primary data set, which is augmented by other mostly high-latitude data compilations. The most recent data come from the Global Temperature and Salinity Profile Program that also includes the Argo global data assembly. We use the EN4 analysis version that employs the Levitus drop rate correction for expandable and mechanical bathythermographs. The two objective analyses (JAMSTEC and EN4) use similar original data but differ in their quality control procedures and objective analysis implementations. We also examine a multisatellite altimeter sea level provided by AVISO on a $1/4^\circ \times 1/4^\circ$ monthly grid for the years 1992–2015.

We examine monthly 10 m equivalent neutral winds from two satellite scatterometers: the NASA SeaWinds scatterometer onboard QuikSCAT (referred to as QuikSCAT) [*Dunbar et al*., 2006] for the period June 1999 to November 2009 and the ASCAT scatterometer onboard the European Meteorological Satellite Organization MetOp-A (referred to as ASCAT) [*Bentamy and Croize-Fillon*, 2012] for the period since 2008. Prior to merging, the ASCAT winds were corrected for the spatial pattern of time mean difference with QuikSCAT during an overlap period 2008–2009, and then the combined data set was mapped onto a uniform $0.5^\circ \times 0.5^\circ$ grid. We use monthly SST data from the NOAA Optimum Interpolation $1/4^\circ$ Daily SST Analysis of *Reynolds et al*. [2007]. Monthly near-surface currents are obtained from the Ocean Surface Current Analyses—Real time (OSCAR) [*Bonjean and Lagerloef*, 2002]. OSCAR estimates horizontal velocity by combining geostrophic velocity from sea surface height, with wind drift. Finally, we also use monthly MODIS-Terra chlorophyll-a concentration (Chl-a) as a proxy for the optical characteristics of near-surface water. Precipitation is provided by the merged-infrared precipitation adjusted by the Tropical Rainfall Measuring Mission data (TRMM product 3B42 version 7). This product spans 50°S–50°N band. Evaporation is provided by the WHOI Objectively Analyzed air-sea Fluxes (OAFlux) [*Yu*, 2007].

To evaluate mixed layer processes such as entrainment and advection, we rely on an eddy-resolving simulation using Parallel Ocean Program (version 2) numerics. The model configuration, similar to that of *Maltrud et al*. [2010] and described in *Grodsky et al*. [2015], has a tripole grid with a nominal resolution of 0.1°. Surface forcing is based on the Coordinated Ocean Reference Experiment atmosphere (COREv2) [*Large and Yeager*, 2004] and climatological monthly river runoff. The simulations begin in 1977 from initial conditions provided by a 15 year spin-up using the exactly repeating "normal year" version of COREv2. Here we examine a 15 year segment of the interannually forced simulations starting from 1994.

The salt budget of the mixed layer is evaluated by vertically averaging the salt transport equation:

$$\underbrace{<\frac{\partial S}{\partial t}>}_{TEND} = -\underbrace{<u\frac{\partial S}{\partial x}>}_{ZADVT} - \underbrace{<v\frac{\partial S}{\partial y}>}_{MADVT} - \underbrace{<w\frac{\partial S}{\partial z}>}_{VADVT} + \underbrace{\frac{(E-P)S}{H}}_{SSF} + \underbrace{\frac{Q_{DIF}(z=H)}{H}}_{VDIF} + <HDIF> \quad (1)$$

where angular brackets, $<>$, denote the vertical average over mixed layer depth (H), S is salinity, E-P is evaporation-minus-precipitation, (u, v, w) is vector velocity, and Q_{DIF} is the diffusive mixing across the base of the mixed layer, $z=H$. The terms in (1) are: salinity tendency (TEND); total zonal (ZADVT), meridional (MADVT), and vertical (VADVT) salinity advection components; normalized surface salt flux (SSF) and vertical diffusion (VDIF) scaled by the mixed layer depth; horizontal diffusion (HDIF). These terms were saved on the original grid at 5 day time resolution. The total salinity advection is further decomposed into two parts such as zonal advection by slowly varying (mean) currents, $\mathrm{ZADV} = <\bar{u} \cdot \partial \bar{S}/\partial x>$, and zonal eddy advection by shorter timescale variations, ZEDDY = ZDAVT − ZDAV. The overbar represents a running 55 day average, which is an effective temporal scale of separation of eddies and seasonal flow in this analysis. This temporal

separation is somewhat arbitrary because the time scale of seasonal forcing and the time scale of mesoscale variability overlap. Our approach of separating by timescale inevitably aliases a portion of eddy contribution into the seasonal currents. HDIF varies on small spatial scales in the open ocean and its contribution to the spatial mean over a *fixed* geographic area is normally negligible.

3. Results

3.1. Observed Changes During 2011–2015

The standard deviation of anomalous SSS is a useful proxy for the magnitude and spatial extent of the highly variable salinity area in the NW Atlantic shelf area (Figure 1). Besides seasonal variations, this area experiences substantial nonseasonal variations. Regardless of the differences in their spatial resolution, both satellite SSS products show that nonseasonal salinity variability is large ($>$0.5 psu) on the Scotian shelf extending southwestward into the MAB. However, north of the Scotian shelf in the area south of the Newfoundland, the two satellite SSS products disagree with weaker variability in the Aquarius product. We attribute this difference to reduced sensitivity over cold water of microwave L band SSS retrievals such as these counteracted in the case of SMOS L4a by the inclusion of in situ observations.

Although there exist some salinity differences associated with the Gulf Stream itself (discussed by *Reul et al*. [2014b]), the maximum of nonseasonal SSS variability area is over the shelf (Figure 1b) and its seaward boundary approximately follows the shelf-slope front, which extends from the Tail of the Grand Banks to Cape Hatteras and separates colder and less saline continental shelf waters from warmer and more saline slope waters. The observed SSS variability may be produced by anomalous shifts of the shelf-slope front, a portion of which is probably associated with latitudinal shifts of the position of the Gulf Stream north wall. Alternatively, the gradients across the shelf-slope front depend on the shelf water characteristics, which in turn depend on water transport from high latitudes. Annual mean OSCAR currents confirm previous findings and show that this fresh and cold water transport takes place through the Scotian Shelf gateway along two main branches of the SSC (Figure 1a). Southwestward transport of Labrador Slope Water passes anticyclonically around the Grand Banks and continues as the SSC offshore branch following along the shelf edge (illustrated with 1000 m depth contour in Figure 1a). The OSCAR currents also resolve another fresh water route that locates just off Nova Scotia coast. This inshore branch of the SSC current is fed by a mixture of waters from the Labrador Shelf and Gulf of St. Lawrence. The two SSC branches eventually merge south of Nova Scotia and carry the high latitude fresh/cold water down into the MAB.

Both advection and frontal shifts induce positively correlated salinity/temperature anomalies, which are detectable in various in situ observation sets [e.g., *Flagg et al*., 2006]. Our satellite SSS confirms that they occupy a significant portion of the shelf extending at least from Nova Scotia and including the MAB (Figure 1). Temporal changes in the observed spatial patterns of anomalous SSS are consistent for the two satellite sensors (Figure 2). Relatively fresh SSS is present south of Nova Scotia during 2011–2012. Coincidently, SMOS shows salty conditions to the north and east in line with the dipole-like pattern revealed by the *Petrie* [2007] analysis. This salty pole is probably obscured in Aquarius data due to the above mentioned degradation in the quality of SSS retrievals over cold waters. SSS increases to its time mean values in 2013. Salinity keeps increasing during 2014 and 2015 (Figure 2).

According to the *Li et al*. [2014] hypothesis, this salinity increase should correspond to stronger than usual southwesterly winds along the seaward coast of Nova Scotia. However, the scatterometer wind anomaly (averaged over the span of satellite SSS records) does not seem to behave like this. Instead, the Scotian coastal wind anomaly is easterly while southeasterly anomalous winds are present over much of the shelf. These anomalous southeasterly winds induce a wind-driven depth-averaged response (directed to the right) with anomalous Ekman currents opposing the prevailing fresh/cold water southwestward transport on the shelf, a factor that may also regulate thermohaline characteristics of the shelf water.

A zero lag Multivariate Empirical Orthogonal Function (EOF) analysis of anomalous SSS and SST (Figure 3) suggests that in the shelf zone south of Nova Scotia temperature and salinity rise in a coherent way during 2011–2015. Indeed, during this period the increase explains 20% of the total variance. Interestingly, this multivariate analysis misses the 2012 SST "heat wave" described by *Mills et al*. [2013]. It was produced by atmospheric blocking events [*Greene and Monger*, 2012], which occurred without a corresponding SSS increase.

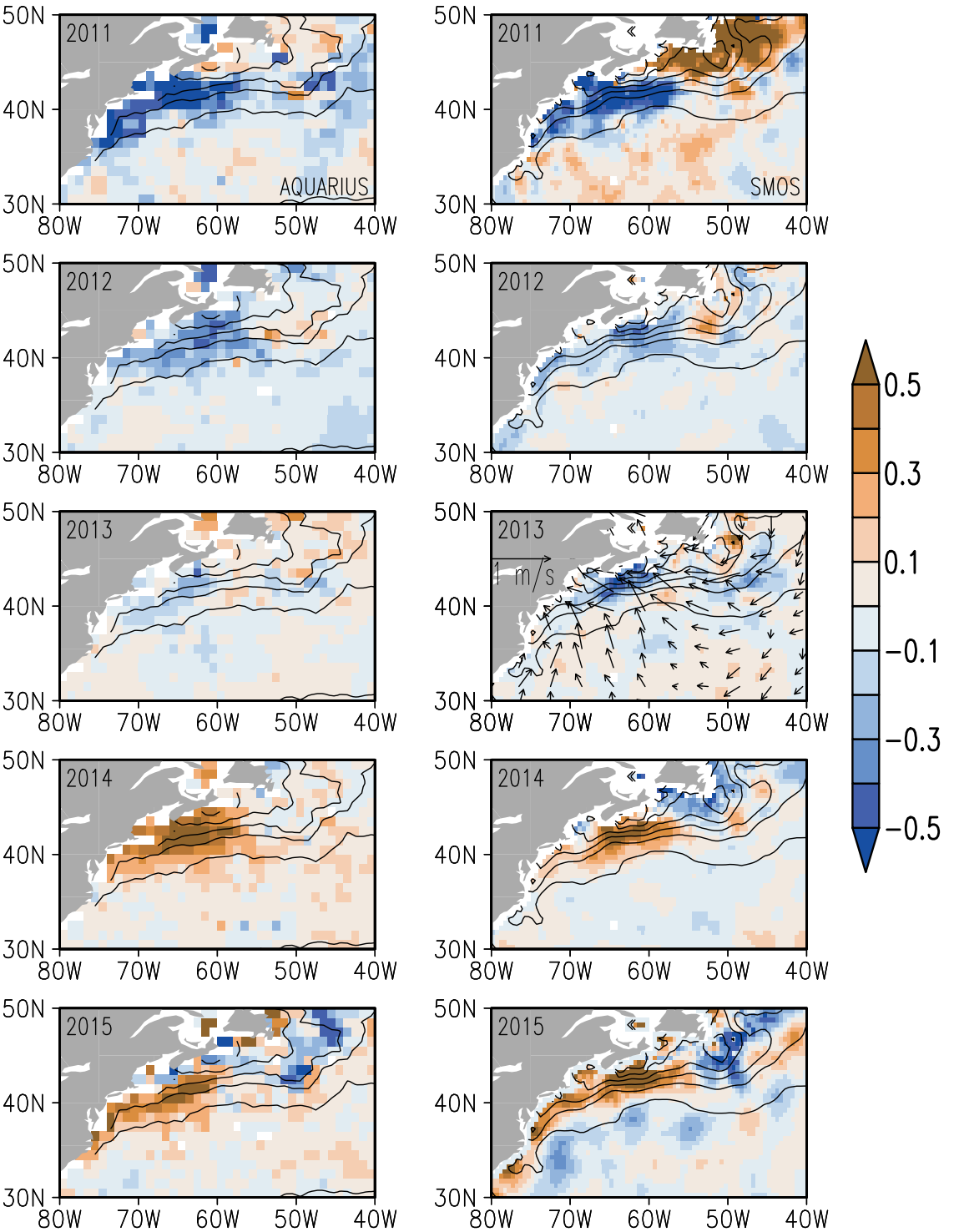

Figure 2. Annually averaged SSS anomaly from (left) Aquarius and (right) SMOS during the Aquarius mission (August 2011 to July 2015). Annual mean SSS contours (32–37 psu, CI = 1-psu) are overlain. 2013 SMOS panel also includes the 2011–2014 mean wind anomaly relative to 1999–2016. Anomalies are calculated with respect to the monthly seasonal cycle.

The gridded analyses of salinity/temperature that we examined capture similarly large spatial scale patterns of SST and SSS (Figure 4). Repeating our multivariate EOF analysis, now including sea level (Figures 4e and 4f) suggests that positive sea level anomalies north of the Gulf Stream wall correlate with salty and warm conditions on the shelf. This correlation may suggest that observed changes are positevely related to shifts in the GSNW latitude (see Figure 4g). Since 2001 the maximum lagged correlation between the GSNW

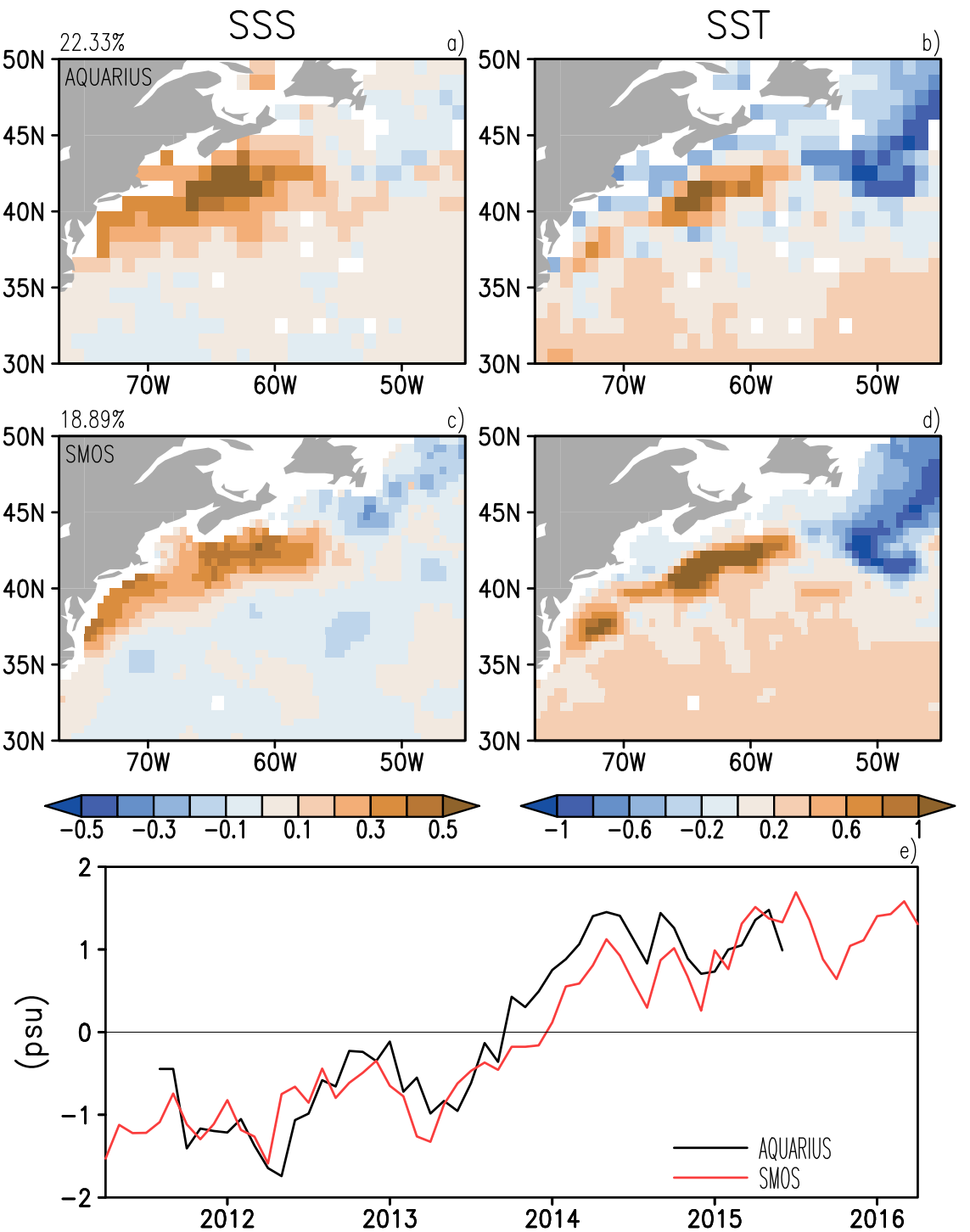

Figure 3. Leading multivariate EOFs of anomalous SSS and SST for (a and b) Aquarius (c and d) SMOS, (e) their corresponding temporal principal components. Percentage of explained variance is shown in Figures 3a and 3c.

latitude and the first principal component time series is about 0.5 (not shown), but salinity variations lead the GSNW latitude shifts by about 4–5 months. Over the longer period (1993–2015), salinity variations on the shelf also lead the GSNW latitude shifts, but the lagged correlation is weaker (~0.35). The latter estimate is line with values reported by *Lee and Lwiza* [2005] and suggests that factors other than Gulf Stream front excursions contribute to the interannual variability of shelf water properties.

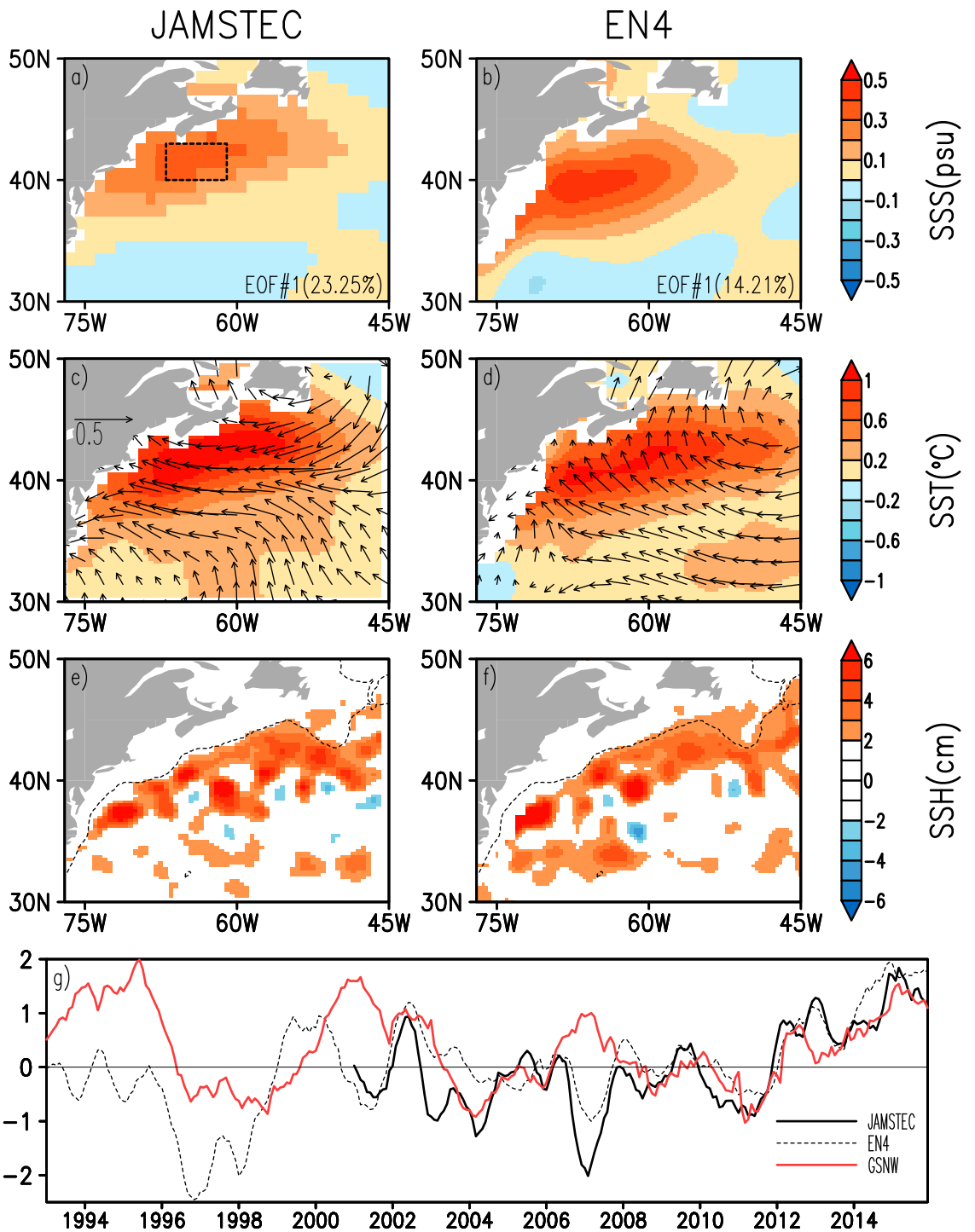

Figure 4. Spatial and temporal components of the leading multivariate EOFs of anomalous monthly SSS, SST (JAMSTEC and EN4 analyses), and SSH (AVISO). Arrows in Figures 4c and 4d are time regression of 6 month average anomalous NCEP/NCAR reanalysis winds [*Kalnay et al.*, 1996] with temporal component of JAMSTEC and EN4 EOFs. (top plots) Percentage of the explained variance is shown. Gulf Stream North Wall (GSNW) latitude anomaly is included in Figure 4g. The 1000 m depth contour is shown in Figures 4e and 4f.

A striking aspect of anomalous temperature and salinity variations on shelf and in the Slope Sea is their large magnitude, spatial coherence, and event-like variations (Figure 4). The strongest event to occur during our period of interest is a cold/fresh anomaly which developed in late 1996 and continued through early 1998. This anomaly had salinities 1.5 psu below normal, the lowest relative salinity in the entire 24 year period of Oleander ship transects [*Flagg et al.*, 2006]. A similarly large event with salinities about 1psu above normal began in 2012 and continues to present (Figures 3 and 4).

3.2. Relation to NAO Events

During 2001–2015, the appearance of warm and salty shelf anomalies occurs coincident with anomalously weak westerly winds (Figure 4c). If the analysis is repeated over the longer period 1993–2015 (using the EN4 analysis), the easterly wind anomaly pattern shifts southeastward (Figure 4d) and is weakly related to salty conditions on the shelf (see also Figure 2 for the wind anomaly during the most recent period of salty conditions on the shelf). These changes are indicative of large-scale shifts in atmospheric patterns, which are likely responsible for adding variance to the Nova Scotia alongshore winds in early, but not recent, decades (discussed in *Li et al*. [2014]). As mentioned above, the wind-driven response induced by this anomalous cross-shelf southeasterly wind decreases the prevailing southwestward fresh/cold water transport on the shelf [see also *Feng et al*., 2016].

As explained in the NOAA Northeast Fisheries Science Center online publication http://www.nefsc.noaa.gov/ecosys/ecosystem-ecology/climate.html (see Figure 1 therein), the strength of zonal winds off Nova Scotia and further south is primarily controlled by the meridional shift of the sea level pressure field between positive and negative phases of the NAO. A positive phase of the NAO denotes a northward shift and increase of westerly winds over the Labrador basin. This northward shift leads (somewhat counterintuitive) to the weakening of prevailing westerly winds to the south. During the negative phase of the NAO, the zonal wind system shifts southward, thus leading to stronger westerly winds east and south of Nova Scotia. Given the correlation pattern in Figure 4c, a positive NAO and thus weaker than normal westerly winds leads to anomalously salty shelf water. From that relationship, one may expect a positive correlation of shelf SSS and the NAO index. In fact, the peak correlation is about 0.5 and corresponds to the NAO leading anomalous SSS by approximately 9 months (Figure 5). Such moderate magnitude of the correlation suggests the involvement of other factors. In particular, *Townsend et al*. [2015] imply that of greater importance than the NAO in recent years are recent increases in freshwater fluxes to the Labrador Sea, which may intensify the volume transport of the inshore, continental shelf limb of the Labrador Current and its continuation as the SSC.

In contrast to the wind correlation patterns (which differ between Figures 4c and 4d), the sea level EOFs (Figures 4e and 4f) suggest a more robust relationship between salty conditions on the shelf and the coastal circulation. For both in situ analyses, sea level shows a positive anomalous seaward gradient across the shelfbreak corresponding to a weakening of the southward geostrophic alongshore currents during salty conditions on the shelf (Figures 4e and 4f).

3.3. The Role of Ocean Circulation

Annual mean near-surface currents (Figure 6a) illustrate the two major pathways of fresh and cold water supply that take place along the shelfbreak (an offshore branch of the SSC) and along the coast (an inshore branch of the SSC). The two branches merge south of Nova Scotia and continue down into the MAB (see also Figure 1a). Currents in the two SSC pathways weaken during salty conditions as shown by the correlation pattern in Figure 6b, which is obtained by projecting the anomalous currents onto the 2001–2015 multivariate leading principal component. This pattern does not change if the 1994–2015 leading principal component (see Figure 4g) is used instead. Note that variations in the outer SSC branch are in line with sea level data in Figures 4e and 4f, but these data do not reproduce variations in the inner SSC branch, which is closer to the coast. Consistent nonseasonal variations in shelf salinity and currents suggest that anomalous cold/freshwater transport by anomalous currents acting on mean salinity gradients play an important role in controlling the water mass properties of the shelf water. The impact of alongshore currents is also evident in the M/V Oleander transects where lower temperatures and salinities are coincident with anomalously strong southwestward alongshore currents [*Flagg et al*., 2006].

The same southwestward alongshore fresh water transport that freshens the shelf also brings nutrients and should result in higher biological productivity. Such expected negative relationship between nonseasonal SSS and Chl-a does occur from shelfbreak extending into the Slope Sea. In this zone, anomalous SSS fluctuations explain only about 20–30% of the standard deviation of anomalous Chl-a. However on the shelf, anomalous Chl-a concentration displays a weak but positive correlation with anomalous SSS (Figure 6b). In part, the lack of correlation between Chl-and SSS may be attributed to seasonality in the regional relationship between the two, which peaks in summer [*Reul et al*., 2014b]. But, assessing the correlation based on summer months only also results in similarly low correlation values (not shown). The weak correlation may also suggest that processes other than advection dominate the Chl-a budget.

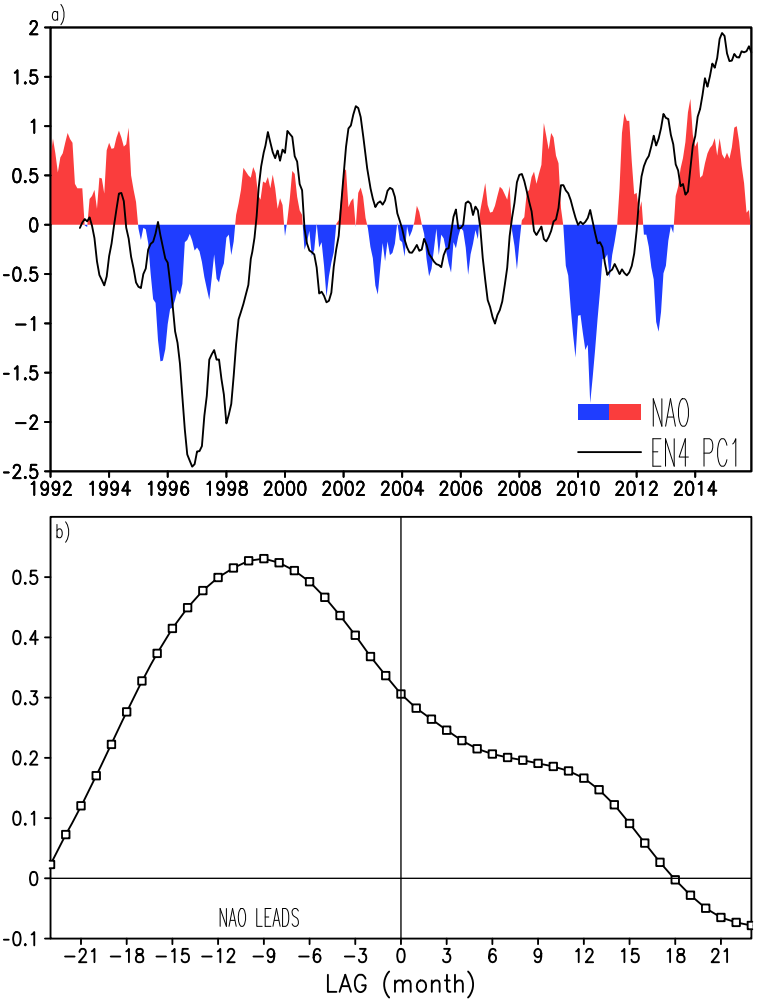

Figure 5. (a) Time series of annually smoothed station-based NAO index [*Hurrell et al.*, 2003] and the leading principal component (PC1) of the EN4 analysis SST, SSS, and SSH (from Figure 4g). (b) Lagged correlation between NAO and PC1.

3.4. Observed Salt Budget

Although the correlation pattern in Figure 6b suggests that southwestward shelf currents weaken during salty events, their relative impact on the salt budget is not apparent. Our empirical evaluation of the salt budget focuses on the Aquarius observations. It is based on the salt budget equation (1) that is vertically averaged within the mixed layer. This allows using the Aquarius SSS as a proxy for vertically averaged salinity. Inevitably, an observation-based analysis does not resolve vertical exchanges (VDIFF + VADV). The horizontal diffusion (HDIFF) normally has fine spatial scales and is averaged out within 1° Aquarius grid. Next, we focus on anomalous salinity budget, which is evaluated for deviations from the climatological monthly seasonal cycle (nonseasonal anomalies). The seasonal cycle is estimated using the reference period (1992–2015), or as much as possible of that available for a particular variable. Anomalous salinity evaluated from relatively short Aquarius data is corrected for the difference in annually average SSS climatology between Aquarius and reference periods using the EN4 data. The anomalous horizontal salinity advection takes the form, where the angular brackets, $< >$, representing vertical averaging are omitted:

$$-(\vec{u}\cdot\nabla S)' = -\vec{u}'\cdot\nabla S - \vec{u}\cdot\nabla S' - \vec{u}'\cdot\nabla S' \quad (2)$$

where "primes" denote anomalies from the climatological monthly cycle. In Figure 7, all terms in (2) are averaged over the Aquarius period 2011–2015. As in Figure 6, mixed layer currents are approximated by the OSCAR currents (referenced to approximately 15 m depth) while mixed layer salinity is approximated by the

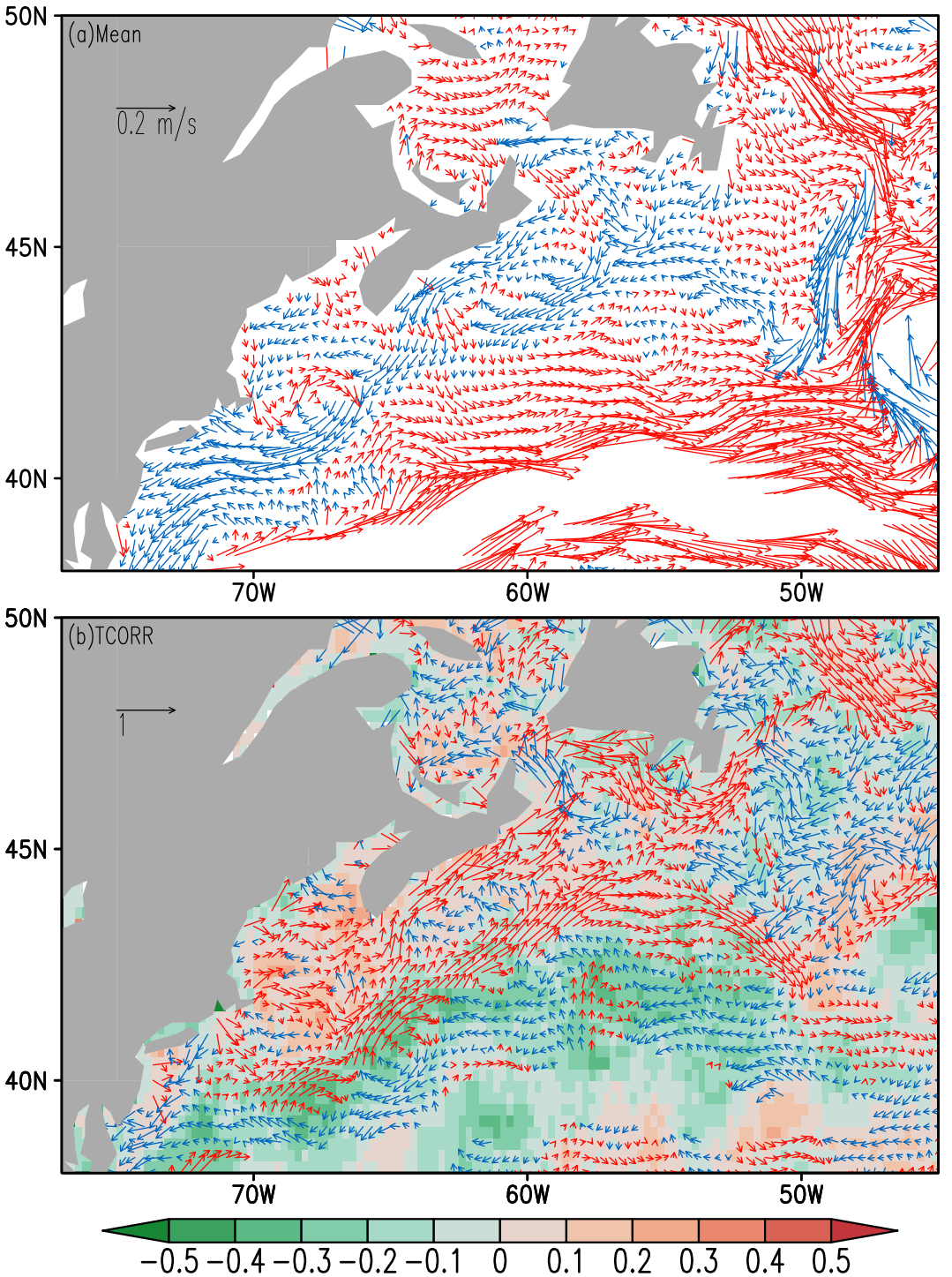

Figure 6. Near-surface currents based on the OSCAR analysis: (a) time mean, (b) vector correlation of the currents with the leading principal component (PC1) of SST, SSS, and SSH for 2001–2015 (Figure 4g). Currents >0.25 m/s are not plotted. Positive/negative values of the zonal current correlation are indicated by red/blue coloring of the arrows. The correlation of PC1 with log(Chl-a) concentration is included in Figure 6b (shading).

Aquarius SSS. The salinity tendency (Figure 7a) resembles the leading EOF shown in Figure 3a reflecting the monotonic increase in SSS at a rate of a few tenths of a psu/year over the period 2011–2015. Normalized net surface salt flux, $SSF=(E-P)S/MLD$, where MLD is the mixed layer depth, is of similar size (Figure 7b). These two terms are almost an order of magnitude weaker than horizontal advection by anomalous

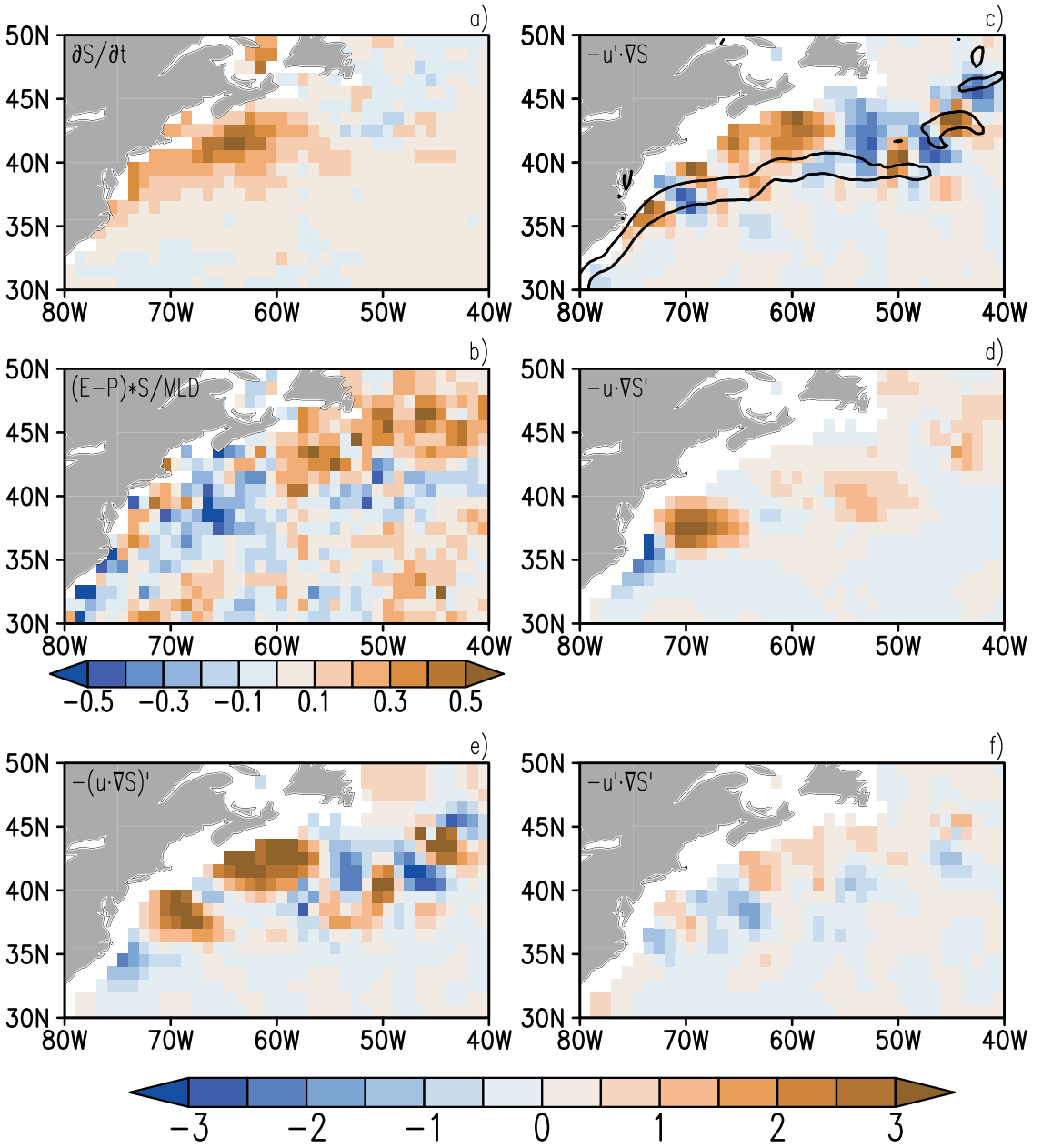

Figure 7. Observation-based anomalous mixed layer salt budget (psu/year) averaged over the Aquarius mission (2011–2015). (a) SSS rate of change, (b) net surface salt flux normalized by mixed layer depth, (c) horizontal salinity advection by anomalous currents, $-\vec{u}' \cdot \nabla S$, (d) horizontal advection of anomalous salinity, $-\vec{u} \cdot \nabla S'$, (e) total anomalous salinity advection $-(\vec{u} \cdot \nabla S)\prime$, (f) anomalous salinity advection by anomalous currents ("eddy-like" term), $-\vec{u}' \cdot \nabla S'$. Color scheme for Figures 7a and 7b is shown below Figure 7b. Color scheme for advection terms is shown at the bottom. Contours in Figure 7c show 0.25 m/s time mean surface currents (a proxy for the Gulfstream position).

currents, $-\vec{u}' \cdot \nabla S$, (Figure 7c). Off Nova Scotia, this advection term dominates the advection of anomalous salinity, $-\vec{u} \cdot \nabla S'$, (Figure 7d), while the latter becomes increasingly important downstream in the MAB. The magnitude of anomalous salinity advection by anomalous currents, $-\vec{u}' \cdot \nabla S'$, is about 20–30% of $-\vec{u}' \cdot \nabla S$ (Figures 7c and 7f). Here one should note that, $-\vec{u}' \cdot \nabla S'$, accounts only for the temporal correlation of non-seasonal anomalies with a characteristic period of month and longer. Although the dominant salinity advection by anomalous currents, $-\vec{u}' \cdot \nabla S$, has a rather complex spatial structure (Figure 7c), we feel what is believable in Figure 7c is the presence of a broad area of positive anomalous salinity advection off Nova Scotia that extends further southwestward and may be an important source of the observed mixed layer salinity increase (Figure 7a). The advection by anomalous currents is negative south of the Newfoundland

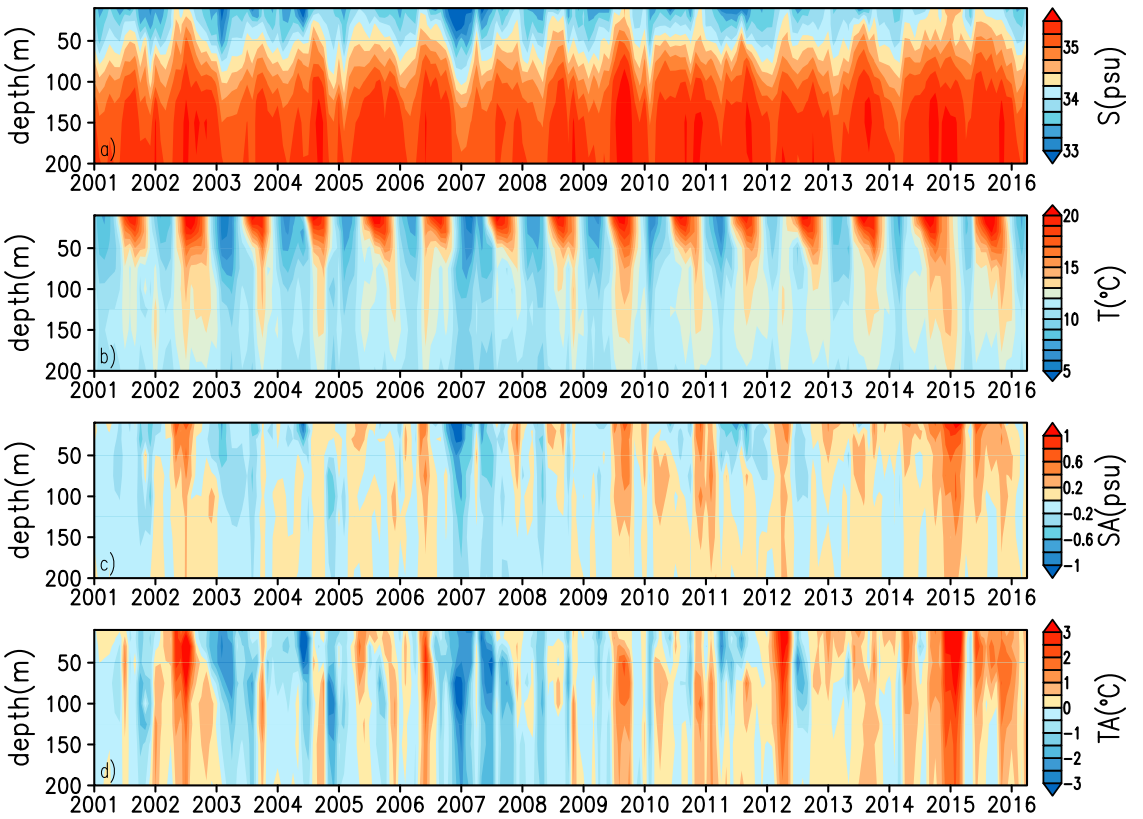

Figure 8. Time-depth diagrams of (a) salinity (S), (b) temperature (T), (c) anomalous salinity (SA), and (d) anomalous temperature (TA) averaged over 67°W–61°W, 40°N–43°N box (see Figure 4a for the box location). Data are based on the JAMSTEC analysis.

that is not apparently present in the mixed layer salinity tendency as estimated from Aquarius (Figure 7a), but does appear in the combined in situ/SMOS L4 SSS analysis (Figure 3c).

Overall, the observation-based salt budget analysis in Figure 7 suggests that salinity advection by anomalous currents, $-\vec{u}' \cdot \nabla S$, is the leading term forcing the observed increase in mixed layer salinity on the Scotian shelf, while advection of mixed layer salinity anomalies, $-\vec{u} \cdot \nabla S'$, may be at play in the MAB. All terms of anomalous salinity advection forcing have a characteristic magnitude of a few psu/year, and thus cannot be balanced either by TEND or SSF, both of which are an order of magnitude weaker. Consequently on interannual timescales, the salinity advection by anomalous currents is likely balanced by vertical exchanges at the base of the mixed layer, a term that we cannot estimate directly from observations.

Further evidence for the dominance of horizontal advection in the anomalous salt budget is provided by the positive relationship between variations in temperature and salinity (Figure 4). Because the mixed layer over the shelf and in the Slope Sea is fresher and warmer than deeper water (Figures 8a and 8b), if vertical exchanges dominated they would produce temperature and salinity anomalies of different signs. In contrast, the dominance of horizontal advection produces anomalies of the same sign, as observed. Also, the depth of the mixed layer varies seasonally between 50 and 100 m (Figures 8a and 8b). The vertical scale of positively correlated temperature and salinity anomalies is at least 2 times larger suggesting that vertical exchanges cannot control this exchange. In particular, the 2011–2015 salinity increase seen in satellite SSS (Figures 2 and 3) progressively deepens and penetrates down to 200 m by the 2015 (Figure 8c). Instrumental ADCP records of *Flagg et al.* [2006] reveal a complex shelfbreak flow system, which shows an along-isobath surface-trapped shelfbreak jet with maximum speeds of about 15 cm/s and a vertical decay scale of ~50 m. But offshore of the shelf-break jet, there is also a 40–50 km wide slope current with larger vertical scale extending down to 300 m and similar velocities as those in the shelfbreak jet.

3.5. Model Analysis

We next consider the anomalous salt budget as represented in the numerical simulations, which also show a remarkable maximum of anomalous SSS variability coaligned with the shelf-slope front (Figure 9a). Over

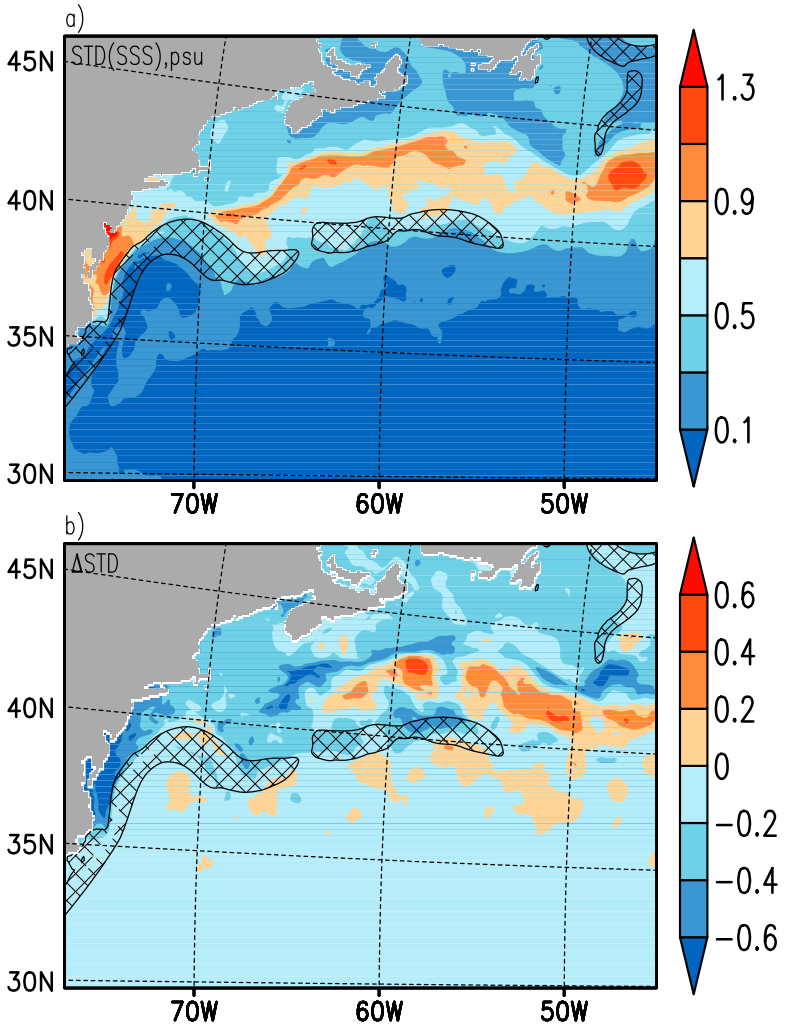

Figure 9. Comparison of standard deviation (STD) of anomalous SSS (periods >1 year) in two model runs forced by interannually varying surface forcing (STD1) and annually repeating surface forcing (STD2, no interannual variations in the forcing). (a) STD1, (b) ΔSTD = STD2-STD1. Annual mean currents >25 cm/s are cross-hatched.

most of the region, the SSS variability is stronger in the ocean forced by interannually varying atmosphere than when the model is driven by annually repeating normal year surface forcing (Figure 9b). But, it is not true in areas surrounding the Gulf Stream that partially intersect the local SSS variability maximum zone located north of the Gulf Stream. In these areas, the intrinsic ocean variability (due to eddies) probably dominates and the lack of interannual (forced) signal does not lead to an expected decrease in SSS variability. The interannually forced ocean dynamics plays an important role in the SSS variability in the NW Atlantic, but its relative impact is spatially dependent and decreases over areas affected by the Gulf Stream eddies. The complex partitioning between the forced and intrinsic ocean variability in this region explains in part the lack of robustness in correlation patterns between observed interannual SSS and winds (Figures 2 and 4c, and 4d). Next, we mainly focus on results from the interannually forced run.

3.5.1. Consistency Between Simulated and Observed Variability

As in the case of the observations presented in Figures (1 and 3), and 4, the dominant EOF of the simulated anomalous SSS is concentrated north of the Gulf Stream and describes positively correlated SSS variations extending southwestward into the MAB (Figure 10a). An SSS increase described by this pattern occurs in phase with warmer SST (Figure 10b). Interestingly, there is a salty and warm stripe extending from the Gulf of St. Lawrence and further southwestward along the seaward coast of the Nova Scotia, which is consistent with the *Li et al.* [2014] hypothesis about the weakening of the inshore branch of the SSC during salt events. The corresponding principal component time series is dominated by 3–5 year time-scale variations that

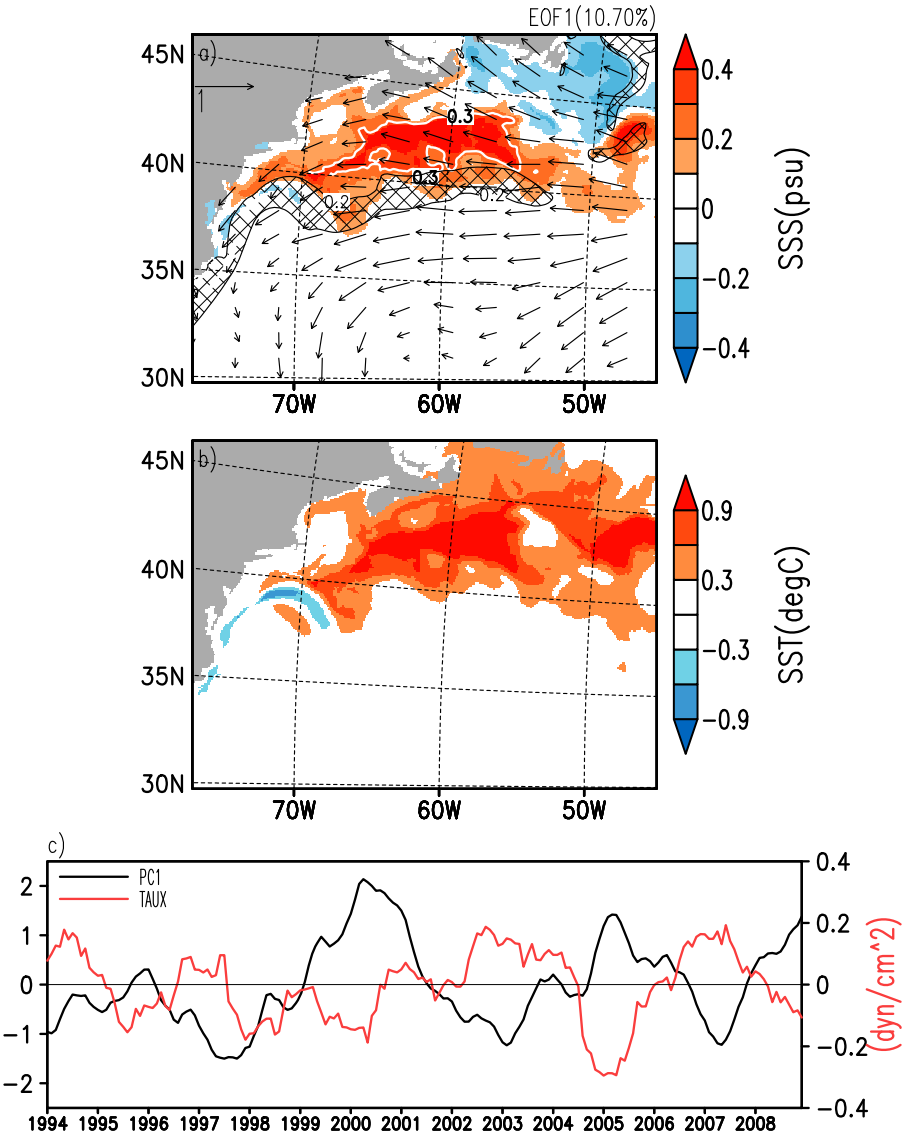

Figure 10. Leading multivariate EOF of monthly anomalous model SSS and SST: (a and b) spatial, (c) temporal components (PC1). In Figure 10a, surface currents >0.2 m/s are cross-hatched, arrows are a temporal correlation of PC1 with 6 month smoothed anomalous wind stress. Anomalous zonal wind stress (TAUX) in Figure 10c is spatially averaged over the index area encompassed by the white contour (0.3 psu) in Figure 10a. It leads PC1 by about 4 months.

follow a weakening of prevailing westerly winds by 4–6 months (Figure 10c). This principal component time series (PC1, Figure 10c) projects on an easterly-southeasterly anomalous wind pattern (Figure 10a) similar to that found in observations (Figure 4c). The wind-driven transport induced by these anomalous winds acts against prevailing southwestward currents on the shelf and the Slope Sea, and thus decreases the transport of fresh/cold water from the high latitudes.

The time mean surface currents in the model (Figure 11a) resemble observations (Figure 6a). The two branches of the SSC are clearly represented. But, some details of simulated currents differ from observations. In particular, some important features of topographically forced circulations around the Grand Banks and Georges Banks are not well resolved in the model. As a result, the offshore branch of the SSC is fed by the Labrador Current extension that circulates south of Newfoundland, rather than encompassing the Grand Banks (as is represented in OSCAR surface currents). Other than those differences, the model does represent the major pathways by which higher latitude surface water is transported down the shelf. The changes in the surface circulation under salty conditions are also in line with the observations presented

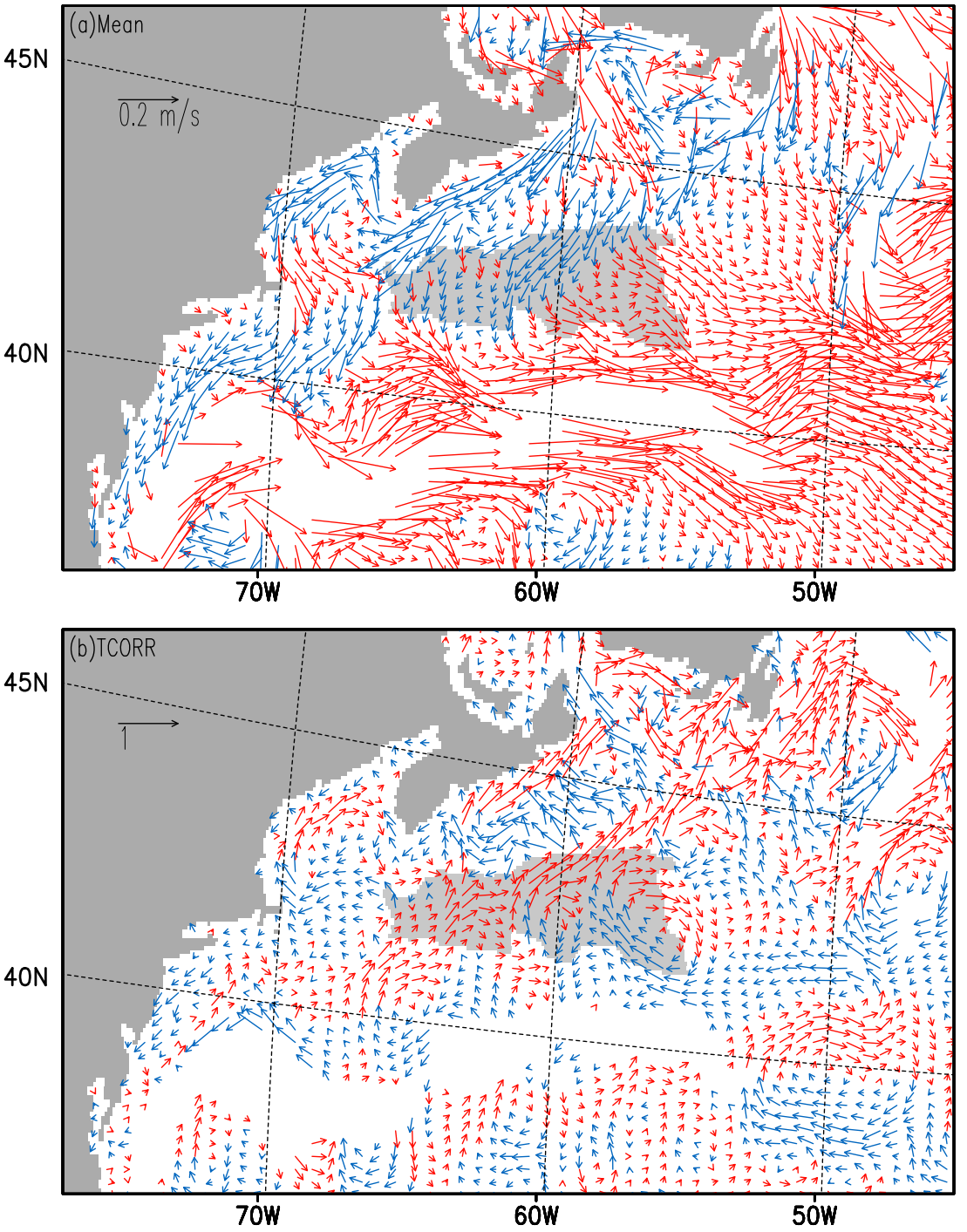

Figure 11. Model coastal currents in the northwestern Atlantic: (a) time mean currents, (b) anomalous currents correlation with temporal part of the leading EOF (PC1, Figure 7c). Areas where currents >0.25 m/s are blanked. Positive/negative zonal component is red/blue, respectively. The index area (see Figure 7a) is shown in light grey.

earlier (Figure 11b). As in the case of the observations (Figure 6b), the two branches of the simulated SSC weaken during salty events. Given the time mean simulated, salt gradient is realistic (not shown), this, in turn, suggests less freshwater transport to areas south of Nova Scotia.

3.5.2. Simulated Salt Budget: Seasonal Analysis

We begin quantification of the nature of salinity variability by focusing on the seasonal cycle in the salinity index area chosen based on the spatial structure of the leading EOF (see the white contour in Figure 10a for the index area location). The model simulates reasonably well the magnitude and annual phase of the

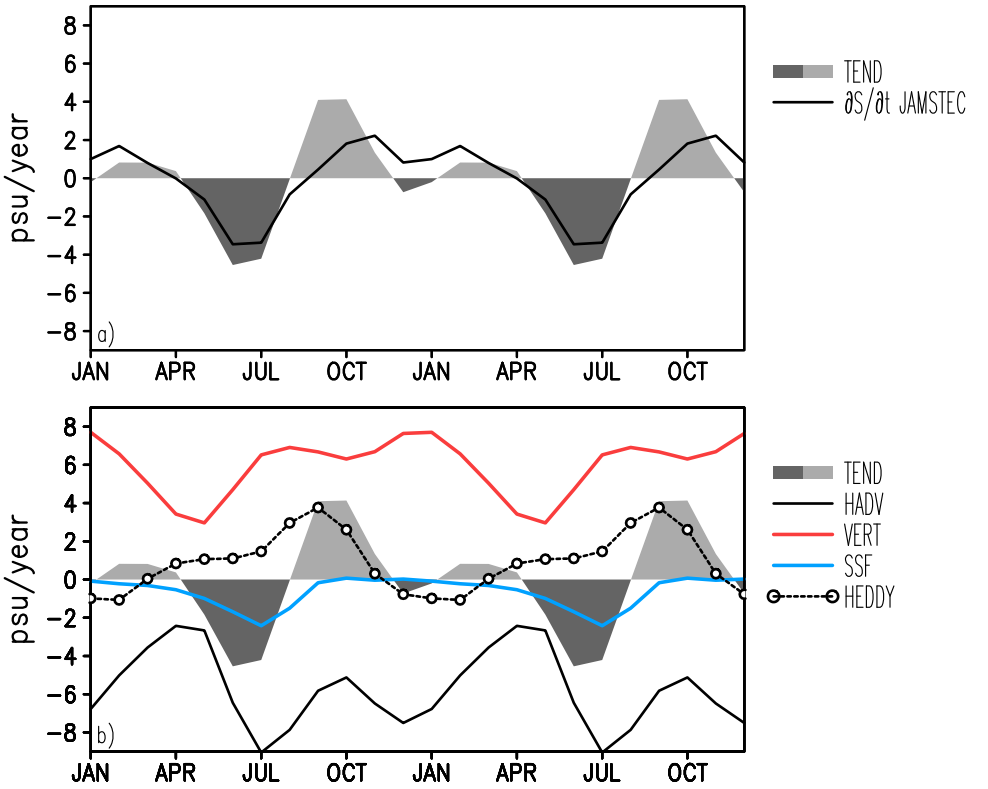

Figure 12. Two years of the seasonal cycle of the simulated mixed layer salt budget terms spatially averaged over the index area shown in Figure 10a: (a) salinity tendency (TEND = $\partial S/\partial t$) and that from JAMSTEC analysis; (b) horizontal salinity advection by mean currents (HADV), vertical processes (vertical advection and turbulent diffusion combined, VERT), surface salt flux normalized by the mixed layer depth (SSF), and horizontal eddy advection (HEDDY).

mixed layer salinity storage, which is in line with the JAMSTEC analysis (Figure 12a). If one exists, the leading forcing term should vary coherently with storage (TEND) and explain its seasonal magnitude and annual phase. However, in the dynamically complex environment adjacent to the Gulf Stream a clearly dominant term is not present. Instead, the seasonal salinity variations are driven by contributions from all terms.

Decomposing the salt budget terms (Figure 12b), we find that seasonal TEND is to some extent driven by horizontal advection by mean currents (HADV), which varies mostly in phase with TEND and has a similar seasonal magnitude. In the shelf and Slope Sea region encompassed by the salinity index area, the mean horizontal salinity advection, HADV, freshens the mixed layer due to the fresh/cold water transport from high latitudes, which seasonal peak occurs in mid-summer. As expected, vertical processes (dominated by the vertical diffusion in the index area) provide mostly salinity flux into the fresh mixed layer and counteract the leading effect of horizontal advection. Because the magnitude of the vertical diffusive flux is proportional to salinity contrast between the mixed layer and saltier water beneath this flux decreases in spring when SSS is at its seasonal maximum. The surface flux term, SSF = $(E-P)S/H$, (see equation (1)) has the smallest but still important seasonal magnitude and is dominated by the effect of summer rainfall. Rainfall in areas adjacent to the Gulf Stream SST front is significant due to the permanent convergence of the near surface winds induced by SST gradients. However, the surface freshwater flux impact is scaled by the mixed layer depth, H, which shrinks in summer, thus leading to the seasonal amplification of the surface flux term, *SSF*. As noted above, our estimate of the horizontal eddy advection may not include the entire effect of the Gulf Stream eddies, because of the fixed separation scale ($\sim$2 months) used in this study. Hence, a portion of the eddy impact may alias into the mean advection, HADV. Horizontal salinity flux by eddies with periods less than 2 months (HEDDY) is mostly positive, which one may expect due to salt/warm Gulf Stream eddies. The eddy-induced salinification of the index area amplifies in fall and opposes the freshening effect of mean currents and displays important seasonal variations with magnitudes comparable to other salt budget terms.

3.5.3. Simulated salt BUDGET: Nonseasonal Analysis

After subtraction of the seasonal variations of each term of (1) and applying a 1 year running mean, we can examine the interannual salt budget (Figure 13). Interannual TEND displays a sequence of oscillations with a characteristic amplitude of about 0.5–1 psu/year suggesting that SSS changes on average by about 1–3 psu between high and low-salinity events, depending on their period (Figure 13b). The rate of change of the mixed layer salinity is explained by the combined action of the total horizontal salinity advection and the vertical exchanges (HADVT+VERT, Figure 13a) while the remaining small difference equals the net surface flux, SSF. Like the seasonal salt budget (Figure 12b), the relative impact of all terms (but the surface flux) on the interannual salinity in the index area is similarly large. However, it can be noted that characteristic magnitude of interannual TEND is smaller than the magnitude of the advection terms. Because TEND generally decreases at longer time scales, this relationship is better seen for a sequence of rather long interannual salinity variations present in the simulations after 1999 (Figure 13b). Disregarding TEND leads to in-phase variations of salinity and the leading forcing term. In fact, local extrema in the horizontal salinity advection by mean currents (HADV, after 1999) roughly corresponds to zero crossings of TEND, and thus occurs almost in phase with salinity extrema (Figures 13a and 13b). For these interannual events, the eddy salinity flux (HEDDY) and vertical exchanges (VERT) tend to act as a negative feedback and are negatively correlated with HADV. The latter governs interannual salinity and leads it by a few months (Figure 13b). This lead is due to the small yet nonnegligible magnitude of TEND.

The leading role of HADV and its in-phase variations with interannual salinity hold for the run long statistics that explains the correlation patterns we see in Figure 11b. Our 15 year simulations produce eight salinity events (Figure 13b). For six of them that develop after mid-1997, the horizontal salinity advection by slowly varying currents (HADV) is the leading forcing term, while the vertical exchanges (VERT) and the horizontal eddy salinity advection (HEDDY) both provide a negative feedback to HADV forcing. Such a balance implies that salinity tendency plays a relatively minor role (the magnitude of TEND is about 20% of that for HADV,

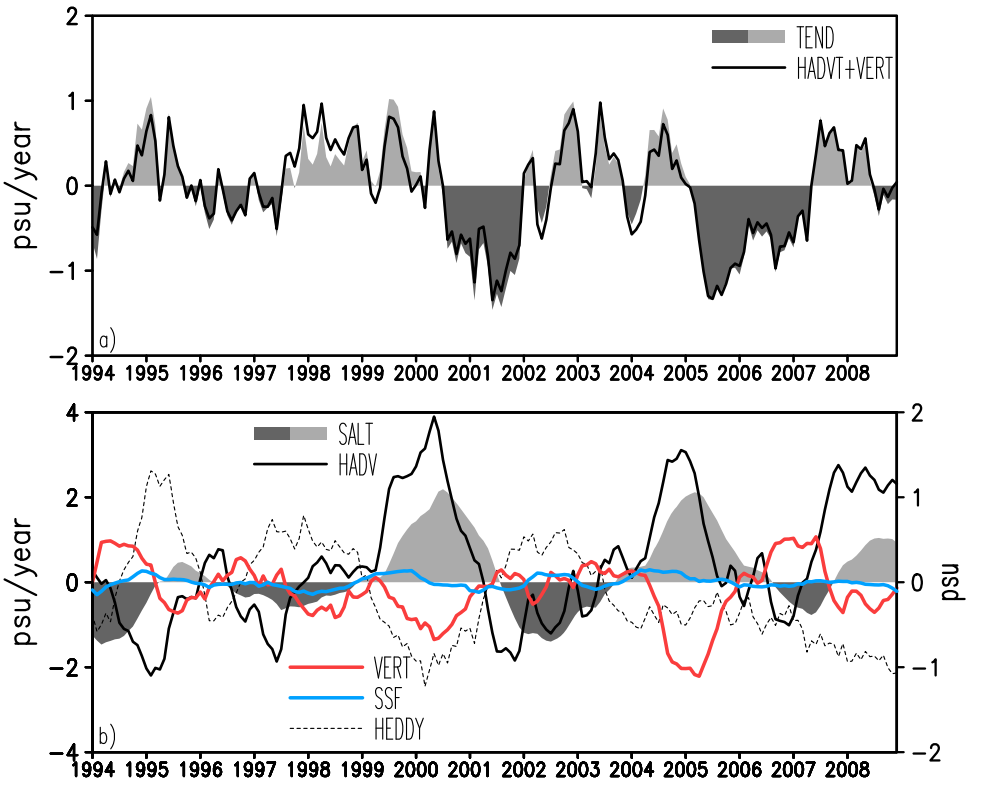

Figure 13. Anomalous mixed layer salt budget terms relative to the seasonal climatology averaged over the index area shown in Figure 7a: (a) salinity tendency (TEND = $\partial S/\partial t$) and the sum of total horizontal advection and vertical processes, (b) horizontal salinity advection by mean currents (HADV), vertical exchanges (vertical advection and turbulent diffusion combined, VERT), surface salt flux normalized by the mixed layer depth (SSF), and horizontal eddy salinity advection (HEDDY).

compare Figures 13a and 13b), and thus interannual salinity varies almost in phase with interannual HADV by slow varying currents. However, the relationship between interannual salinity and advection terms is more complex for events prior to the mid-1997, for which HEDDY acts as a leading forcing (Figure 13b). This suggests that eddy shedding by the Gulf Stream and the role they play in the interannual salt balance of the Slope Sea are also important, as one may expect in this dynamically complex region. Gross negative correlation between the eddy and mean horizontal salinity transport (Figure 13b) is a very striking characteristic also present in other eddy resolving ocean simulations at various time scales [e.g., *Treguier et al*., 2012]. Interannual variations of the surface salt flux are weak in comparison with other terms and their contribution can be quantified as negligible (Figure 13b).

4. Summary and Discussion

During the Aquarius and SMOS satellite missions (2011–2015), SSS displays a steady and consistent increase of about 1 psu over the entire NW Atlantic shelf area south of Nova Scotia. These SSS changes are in part related to the weakening of the ocean shelf currents in turn induced by changes in the atmospheric circulation due to a strengthening of the NAO during this period. Comparing the results from this short 5 year period with a similar examination of two historical in situ-based ocean profile data analyses (from JAMSTEC and Hadley Centre, EN4) indicates that mixed layer salinity and temperature north of the Gulf Stream experience positively correlated interannual oscillations at a rate of 1 psu per 2°C, which have shelf-wide spatial patterns and that these salty and warm events are coincident with an easterly-southeasterly wind anomaly over the shelf. The presence of these positively correlated anomalies suggests a key role for horizontal advection rather than vertical exchanges (the latter would have led to negatively correlated anomalies).

About 50% of interannual SSS variability can be related to interannual variations of the NAO index and related meridional shifts of the North Atlantic wind patterns, which lead anomalous SSS on the shelf by about 9 months. The wind systems shift northward during NAO+ that leads to weakening zonal winds off and to the south of Nova Scotia. The wind weakening forces anomalous Ekman transport that acts in the opposite direction of the mean shelf currents (which are directed southwestward), which supply cold/fresh water from the north. The OSCAR near-surface current analysis shows that these events are coincident with the weakening of both branches of the Scotian Shelf Current (SSC). But, they correlate only moderately with the latitude of the Gulf Stream North Wall. This suggests that salinity advection by anomalous currents in the SSC acting on the mean salinity gradient is the primary forcing that regulates the appearance of fresh/cold anomalies in shelf area extending from Nova Scotia down to the Mid-Atlantic Bight. This forcing has a characteristic magnitude of a few psu/year, and thus cannot be balanced either by surface salt flux or salinity tendency, which are an order of magnitude weaker. Since storage is much smaller than anomalous horizontal salinity advection on interannual timescales, this advection term is mostly balanced by vertical exchanges.

Positively correlated interannual salinity and temperature oscillations over the entire NW Atlantic shelf area is also a characteristic of our eddy resolving ocean model simulations. The model salt budget confirms that interannual horizontal salinity advection is the main driver of interannual salinity, while the vertical exchanges provide negative feedback. Contributions from horizontal diffusion and net surface salt flux are small. TEND plays a relatively minor role on interannual periods (the magnitude of interannual TEND is about 20% of horizontal advection), and thus interannual salinity varies almost in phase with interannual HADV. Fifteen year-long simulations produce eight interannual salinity oscillations (positive and negative). Six of them are driven by the horizontal advection by slow varying currents ($>$2 months), while two events are driven by the horizontal eddy advection ($<$2 months). This suggests that eddy shedding by the Gulf Stream and the role that the eddies play in the interannual salt balance of the Slope Sea is nonnegligible, as one may expect in this dynamically complex region. As in the case of our observational analysis, the simulations show salt/warm events are connected with southeasterly wind anomalies over the shelf and anomalously weak Scotian Shelf Current and that such wind anomalies are the main mechanism by which fresh high latitude water is transported west southwestward along the shelf.

Shifts in the water mass properties of the shelf water inevitably shift the spatial and temporal distribution of marine populations because of thermal preferences. The new satellite observations discussed in this paper allow for better evaluation of SSS and SST gradients, and thus improve our ability to monitor the advection

of salt and heat into this region. Adding satellite SSS to the existing suite of tools for ocean remote sensing will also open up further studies. Possibilities include the use of SSS as a tracer (jointly with SST) of the role of currents in producing warm, salty, and poor Chl water on the shelf and their links with large-scale atmosphere variability and biological response.

Acknowledgments
This research was supported by NASA: NNX12AF68G and NNX15AG40G to UMD, and NNX10AC16G to NCAR. F.B. was also supported by the NSF through its sponsorship of the NCAR. Computing resources were provided by the Computational and Information Systems Laboratory of NCAR. William Boicourt comments and discussions were extremely helpful. SSALTO/DUACS altimetry is produced by AVISO with support from CNES (www.aviso.altimetry.fr/duacs/). Aquarius SSS is available at ftp://podaac-ftp.jpl.nasa.gov/allData/aquarius/L3/mapped/V4/daily/SCI/. MODIS-Terra Chlorophyll is provided by the NASA GSFC Ocean Biology Processing Group (doi:10.5067/TERRA/MODIS/L3M/CHL/2014, oceandata.sci.gsfc.nasa.gov/MODIS-Terra/Mapped). SMOS L4a data are available at http://www.ifremer.fr/naiad/salinityremotesensing.ifremer.fr/CEC_Products/. QuikSCAT and ASCAT winds are available at ftp://podaac-ftp.jpl.nasa.gov/OceanWinds/quikscat/L3/jpl/v2/hdf/ and ftp://ftp.ifremer.fr/ifremer/cersat/products/gridded/MWF/L3/ASCAT, respectively. OSCAR currents are available at podaac.jpl.nasa.gov/dataset/OSCAR_L4_OC_third-deg. TRMM 3B42 (version 7) rainfall was obtained from disc.sci.gsfc.nasa.gov/precipitation/. OAFlux evaporation is distributed via oaflux.whoi.edu/evap.html.

References

Andres, M. (2016), On the recent destabilization of the Gulf Stream path downstream of Cape Hatteras, *Geophys. Res. Lett.*, *43*, 9836–9842, doi:10.1002/2016GL069966.

Beardsley, R. C., and W. C. Boicourt (1981), On estuarine and continental-shelf circulation in the Middle Atlantic Bight, in *Evolution of Physical Oceanography, Scientific Surveys in Honor of Henry Stommel*, edited by B. A. Warren and C. Wunsch, pp. 198–233, MIT Press, Cambridge, Mass.

Bentamy, A., and D. Croize-Fillon (2012), Gridded surface wind fields from Metop/ASCAT measurements. *Int. J. Remote Sens.*, *33*, 1729–1754.

Bisagni, J. J., H.-S. Kim, and A. Chaudhuri (2009), Interannual variability of the shelf-slope front position between 75 degrees and 50 degrees W, *J. Mar. Syst.*, *78*(3) 337–350.

Bonjean, F., and G. S. E. Lagerloef (2002), Diagnostic model and analysis of the surface currents in the tropical pacific ocean, *J. Phys. Oceanogr.*, *32*, 2938–2954, doi:10.1175/1520-0485(2002)032 < 2938:DMAAOT>2.0.CO;2.

Boutin, J., N. Martin, X. Yin, J. Font, and N. Reul (2012), First Assessment of SMOS Data Over Open Ocean: Part II-sea surface salinity, *IEEE Trans. Geosci. Remote Sens.*, *50*(5), 1662–1675, doi:10.1109/TGRS.2012.2184546.

Boutin, J., N. Martin, N. Kolodziejczyk, and G. Reverdin (2016), Interannual anomalies of SMOS sea surface salinity, *Remote Sens. Environ.*, *180*, 128–136, doi:10.1016/j.rse.2016.02.053.

Chapman, D. C., J. A. Barth, R. C. Beardsley, and R. G. Fairbanks (1986), On the continuity of mean flow between the Scotian Shelf and the Middle Atlantic Bight, *J. Phys. Oceanogr.*, *16*(4), 758–772, doi:10.1175/1520-0485(1986)016<0758:OTCOMF>2.0.CO;2.

Csanady, G.T. and P. Hamilton (1988), Shelf edge exchange processes of the mid-Atlantic bight circulation of slopewater, *Cont. Shelf Res.*, *8*(5), 565–624, doi:10.1016/0278-4343(88)90068-4.

Dunbar, S., et al. (2006), QuikSCAT Science Data Product User Manual, Version 3.0, JPL Doc. D-*18053: Rev A*, Jet Propul. Lab., Pasadena, Calif. [Available at ftp://podaac-ftp.jpl.nasa.gov/allData/quikscat/L2B/docs/QSUG_v3.pdf.]

Ezer, T. and Atkinson, L. P. (2014), Accelerated flooding along the U.S. East Coast: On the impact of sea-level rise, tides, storms, the Gulf Stream, and the North Atlantic Oscillations, *Earth Future*, *2*, 362–382, doi:10.1002/2014EF000252.

Feng, H., D. Vandemark, and J. Wilkin (2016), Gulf of Maine salinity variation and its correlation with upstream Scotian Shelf currents at seasonal and interannual time scales, *J. Geophys. Res. Oceans*, *121*, 8585–8607, doi:10.1002/2016JC012337.

Flagg, C. N., M. Dunn, D.-P. Wang, H. T. Rossby, and R. L. Benway (2006), A study of the currents of the outer shelf and upper slope from a decade of shipboard ADCP observations in the Middle Atlantic Bight, *J. Geophys. Res.*, *111*, C06003, doi:10.1029/2005JC003116.

Foltz, G. R., S. A. Grodsky, J. A. Carton, and M. J. McPhaden (2004), Seasonal salt budget of the northwestern tropical Atlantic Ocean along 38°W, *J. Geophys. Res.*, *109*, C03052, doi:10.129/2003JC0021112004.

Gawarkiewicz, G. G., R. E. Todd, A. J. Plueddemann, M. Andres, and J. P. Manning (2012), Direct interaction between the Gulf Stream and the shelfbreak south of New England. *Sci. Rep. 2*, 553, doi:10.1038/srep00553.

Good, S. A., M. J. Martin, and N. A. Rayner (2013), EN4: Quality controlled ocean temperature and salinity profiles and monthly objective analyses with uncertainty estimates, *J. Geophys. Res. Oceans*, *118*, 6704–6716, doi:10.1002/2013JC009067.

Greene, C. H., and B. C. Monger (2012), An Arctic wild card in the weather, *Oceanography*, *25*(2), 7–9, doi:10.5670/oceanog.2012.58.

Greene, C. H., et al. (2013), Remote climate forcing of decadal-scale regime shifts in Northwest Atlantic shelf ecosystems, *Limnol. Oceanogr.*, *58*(3), 803–816, doi:10.4319/lo.2013.58.3.0803.

Grodsky, S. A., N. Reul, G. S. E. Lagerloef, G. Reverdin, J. A. Carton, B. Chapron, Y. Quilfen, V. N. Kudryavtsev, and H.-Y. Kao (2012), Haline hurricane wake in the Amazon/Orinoco plume: AQUARIUS/SACD and SMOS observations, *Geophys. Res. Lett.*, *39*, L20603, doi:10.1029/2012GL053335.

Grodsky, S. A., B. K. Johnson, J. A. Carton, and F. O. Bryan (2015), Interannual Caribbean salinity in satellite data and model simulations, *J. Geophys. Res. Oceans*, *120*, 1375–1387, doi:10.1002/2014JC010625.

Hosoda, S., T. Ohira, and T. Nakamura (2008), A monthly mean dataset of global oceanic temperature and salinity derived from Argo float observations, *JAMSTEC Rep. Res. Dev.*, *8*, 47–59. [Available at http://www.jamstec.go.jp/ARGO/argo_web/MapQ/Hosoda_etal_MOAA_GPV.pdf.]

Houghton, R., and R. Fairbanks (2001), Water sources for Georges Bank, *Deep Sea Res., Part II*, *48*(1), 95–114, doi:10.1016/S0967-0645(00)00082-5.

Hurrell, J. W., Y. Kushnir, G. Ottersen, and M. Visbeck (2003), The North Atlantic oscillation: Climatic significance and environmental impact, in *An Overview of the North Atlantic Oscillation, Geophys. Monogr. Ser.*, vol. 134, edited by J. W. Hurrell et al., pp. 1–35, AGU, Washington, D. C.

Joyce, T. M., C. Deser, and M. A. Spall (2000), The relation between decadal variability of subtropical mode water and the North Atlantic oscillation, *J. Clim.*, *13*(14), 2550–2569.

Kalnay, E., and Coauthors (1996), The NCEP/NCAR 40-year reanalysis project, *Bull. Amer. Meteor. Soc.*, *77*, 437–471.

Lagerloef, G., F. Wentz, S. Yueh, H.-Y. Kao, G. C. Johnson, and J. M. Lyman (2012), Aquarius satellite mission provides new, detailed view of sea surface salinity, in State of the Climate 2011, *Bull. Am. Meteorol. Soc.*, *93*(7), S70–S71.

Large, W. G., and S. G. Yeager (2004), Diurnal to decadal global forcing for ocean and sea-ice models: The datasets and flux climatologies, NCAR Tech. Note TN-460+STR, Natl. Cent. for Atmos. Res., Boulder, Colo.

Lee, T. (2016), Consistency of Aquarius sea surface salinity with Argo products on various spatial and temporal scales, *Geophys. Res. Lett.*, *43*, 3857–3864, doi:10.1002/2016GL068822.

Lee, Y. J., and K. Lwiza (2005), Interannual variability of temperature and salinity in shallow water: Long Island Sound, New York, *J. Geophys. Res.*, *110*, C09022, doi:10.1029/2004JC002507.

Lentz, S. J. (2010), The mean along-isobath heat and salt balances over the middle atlantic bight continental shelf, *J. Phys. Oceanogr.*, *40*(5), 934–948.

Li, Y., R. Ji, P. S. Fratantoni, C. Chen, J. A. Hare, C. S. Davis, and R. C. Beardsley (2014), Wind-induced interannual variability of sea level slope, alongshelf flow, and surface salinity on the Northwest Atlantic shelf, *J. Geophys. Res. Oceans*, *119*, 2462–2479, doi:10.1002/2013JC009385.

Linder, C. A., and G. Gawarkiewicz (1998), A climatology of the shelfbreak front in the Middle Atlantic Bight. *J. Geophys. Res.*, *103*, 18,405–18,423.
Liu, H., S. A. Grodsky, and J. A. Carton (2009), Observed subseasonal variability of oceanic barrier and compensated layers, *J. Clim.*, *22*, 6104–6119, doi:10.1175/2009JCLI2974.1.
Loder, J. W., W. C. Boicourt, and J. H. Simpson (1998a), Overview of western ocean boundary shelves, in *The Global Coastal Ocean: Regional Studies and Synthesis. The Sea*, vol. 11, edited by A. R. Robinson and K. H. Brink, chap. 1, pp. 3–27, John Wiley, New York.
Loder, J. W., Petrie, B., and Gawarkiewicz, G. (1998b), The coastal ocean off northeastern North America: A large-scale view, in: *The Global Coastal Ocean: Regional Studies and Synthesis. The Sea*, vol. 11, edited by: A. R. Robinson and K. H. Brink, John Wiley, New York.
Loder, J. W., J. A. Shore, C. G. Hannah, and B. D. Petrie (2001), Decadal-scale hydrographic and circulation variability in the Scotia–Maine region, *Deep Sea Res., Part II*, *48*(1), 3–35.
Maltrud, M., F. Bryan, and S. Peacock (2010), Boundary impulse response functions in a 681 century-long eddying global ocean simulation, *Environ. Fluid Mech.*, *10*, 275–295 doi:10.1007/s10652-009-9154-3.
Melnichenko, O., P. Hacker, N. Maximenko, G. Lagerloef, and J. Potemra (2016), Optimum interpolation analysis of Aquarius sea surface salinity, *J. Geophys. Res. Oceans*, *121*, 602–616, doi:10.1002/2015JC011343.
Mills, K. E., et al. (2013), Fisheries management in a changing climate: Lessons from the 2012 ocean heat wave in the Northwest Atlantic, *Oceanography*, *26*(2), 191–195, doi:10.5670/oceanog.2013.27.
Petrie, B. (2007), Does the north Atlantic oscillation affect hydrographic properties on the Canadian Atlantic continental shelf?, *Atmos. Ocean*, *45*(3), 141–151, doi:10.3137/ao.450302.
Petrie, B., and K. Drinkwater (1993), Temperature and salinity variability on the Scotian Shelf and in the Gulf of Maine 1945–1990, *J. Geophys. Res.*, *98*, 20,079–20,089.
Reul, N., et al. (2014a), Sea surface salinity observations from space with the SMOS satellite: A new means to monitor the marine branch of the water cycle, *Surv. Geophys.*, *35*, 681–772, doi:10.1007/s10712-013-9244-0.
Reul, N., B. Chapron, T. Lee, C. Donlon, J. Boutin, and G. Alory (2014b), Sea surface salinity structure of the meandering Gulf Stream revealed by SMOS sensor, *Geophys. Res. Lett.*, *41*, 3141–3148, doi:10.1002/2014GL059215.
Reul, N., J. Tenerelli, and S. Guimbard (2015), SMOS Level 3 &4 Research products of the Centre d'Expertise Ifremer du CATDS: Algorithm Theoretical Background Document, *Tech. Rep. 1*, IFREMER. [Available at http://www.ifremer.fr/naiad/salinityremotesensing.ifremer.fr/CEC_Products/Documentation/CATDS_CECOS_SMOS_Level4aProducts_ATBD.pdf.]
Reynolds, R. W., T. M. Smith, C. Liu, D. B. Chelton, K. S. Casey and M. G. Schlax (2007), Daily high-resolution blended analyses for sea surface temperature, *J. Clim.*, *20*, 5473–5496.
Rossby, T. (1999), On gyre interactions, *Deep Sea Res., Part II*, *46*, 139–164.
Saba, V. S., K. J. W. Hyde, N. D. Rebuck, K. D. Friedland, J. A. Hare, M. Kahru, and M. J. Fogarty (2015), Physical associations to spring phytoplankton biomass interannual variability in the U.S. Northeast Continental Shelf, *J. Geophys. Res. Biogeosci.*, *120*, 205–220, doi:10.1002/2014JG002770.
Sanchez-Franks, A., S. Hameed, and R. E. Wilson (2016), The icelandic low as a predictor of the gulf stream north wall position, *J. Phys. Oceanogr.*, *46*(3), 817–826, doi:10.1175/JPO-D-14-0244.1.
Schollaert, S. E., T. Rossby, and J. A. Yoder (2004), Gulf Stream cross-frontal exchange: Possible mechanisms to explain interannual variations in phytoplankton chlorophyll in the Slope Sea during the SeaWiFS years, *Deep Sea Res., Part II*, *51*(1–3), 173–188.
Taylor, A. H., and J. A. Stephens (1998), The North Atlantic Oscillation and the latitude of the Gulf Stream, *Tellus Ser. A*, *50*, 134–142, doi:10.1034/j.1600-0870.1998.00010.x.
Townsend, D. W., A. C. Thomas, L. M. Mayer, M. A. Thomas, and J. A. Quinlan (2006), Oceanography of the Northwest Atlantic Continental Shelf, in *The Sea: The Global Coastal Ocean: Interdisciplinary Regional Studies and Syntheses*, edited by A. R. Robinson and K. H. Brink, Harvard Univ. Press, Cambridge, Mass.
Townsend, D. W., N. R. Pettigrew, M. A. Thomas, M. G. Neary, D. J. McGillicuddy Jr., and J. O'Donnell (2015), Water masses and nutrient sources to the Gulf of Maine, *J. Mar. Res.*, *73*(3–4), 93–122, doi:10.1357/002224015815848811.
Treguier, A. M., J. Deshayes, C. Lique, R. Dussin, and J. M. Molines (2012), Eddy contributions to the meridional transport of salt in the North Atlantic, *J. Geophys. Res.*, *117*, C05010, doi:10.1029/2012JC007927.
Umbert, M., S. Guimbard, G. Lagerloef, L. Thompson, M. Portabella, J. Ballabrera-Poy, and A. Turiel (2015), Detecting the surface salinity signature of Gulf Stream cold-core rings in Aquarius synergistic products, *J. Geophys. Res. Oceans*, *120*, 859–874, doi:10.1002/2014JC010466.
Wen, N., Z. Liu, Q. Liu, and C. Frankignoul (2005), Observations of SST, heat flux and North Atlantic Ocean-atmosphere interaction, *Geophys. Res. Lett.*, *32*, L24619, doi:10.1029/2005GL024871.
Wills, S. M., D. W. J. Thompson, and L. M. Ciasto (2016), On the Observed Relationships between variability in Gulf stream sea surface temperatures and the atmospheric circulation over the North Atlantic, *J. Clim.*, *29*, 3719–3730, doi:10.1175/JCLI-D-15-0820.1.
Yu, L. (2007), Global variations in oceanic evaporation (1958-2005): The role of the changing wind speed. *J. Clim.*, *20*(21), 5376–5390.